

TABLE 6
Clinical Features of Long-Term Survivors

NYHA	Class I	6
	Class II	1 (cyanosis, arrhythmia)
SpO ₂ (%)		88.8 ± 6.8
Hemodynamic Indices		
	mPAP (mmHg)	11.0 ± 2.6
	PCWP (mmHg)	5.8 ± 2.0
	SVEDVI (ml/m ²)	104 ± 37
	SVEF (%)	52.0 ± 6.5

PAP = pulmonary artery pressure; PCWP = pulmonary capillary wedge pressure; SVEDVI = single ventricular end diastolic volume index; SVEF = single ventricular ejection fraction.

saturation was 88.8 ± 6.8%. The hemodynamic indices were also sufficient to allow participation in the activities of daily life. The average pulmonary arterial pressure for the patients was 11.0 ± 2.6 mmHg, pulmonary capillary wedge pressure was 5.8 ± 2.0 mmHg, single ventricular end diastolic volume index was 104 ± 37 mL/m², and the SVEF was 52.0 ± 6.5%.

DISCUSSION

The surgical treatment of atrial isomerism patients aiming for UVR is challenging, and the long-term outcome after a Fontan completion is still unclear. In the present paper, we describe the long-term clinical features of atrial isomerism patients who adjusted to Fontan circulation.

In this series, life-threatening problems still remained 10 years after the Fontan completion in spite of achieving excellent outcome for the first several years after UVR. In particular, all of the expired patients had a single right ventricle (SRV) and all but one expired due to ventricular failure. Although our data did not confirm it to the level of statistical significance, we cannot renounce the possibility that the SRV cannot tolerate the systemic circulation over the years, as has been previously reported.¹⁰⁻¹³

The staging Fontan strategy was the independent predictor of long-term survival after the Fontan completion. It is well known that this strategy enables relatively younger patients to reduce the ventricular volume load and attenuate cyanosis before the completion of adaptation to Fontan circulation. In addition, Tanoue et al. clearly explained that this strategy improved the ventricular energetics after TCPC.¹⁴ We speculate that these effects help to maintain good Fontan circulation long after UVR.

TCPC, as an alternative to the conventional Fontan type procedure, can keep the coronary sinus in the low pressure atrium, thereby contributing to the protection of ventricular function.¹⁵ The introduction of EC-TCPC enabled isomerism patients who had complex systemic venous drainage to receive this benefit.¹⁵ Also, Hsia et al. revealed that TCPC contributed reduction of loss of energy by creating laminar blood flow.¹⁶ For these reasons, we consider that the EC-TCPC was the other independent predictor of long-term survival.

Although it is well known that AT is a serious major problem, particularly in right atrial isomerism hearts, because of the disposition of the conduction system,^{17,18} there was no statistically significant relationship between long-term mortality and arrhythmia. In this series, we included two long-term survivors who converted from the conventional Fontan type operation to EC-TCPC because of the occurrence of AT and successfully recovered sinus rhythm. The EC-TCPC procedure has an isolated advantage over any other Fontan modification because it prevents right atrial dilatation and reduces the occurrence of atrial tachyarrhythmia (AT).¹⁹ The initiation of EC-TCPC undoubtedly diminished this risk, even in the isomerism patients.

Postoperative CAVR was seen in half of the expired patients and was found to be a risk factor of long-term survival. We considered that even if CAVR was repaired, until the Fontan completion and Fontan circulation was successfully established, the native CAVV competence would thus influence the long-term mortality.

Study limitations

In this study, we excluded early and mid-term mortalities after the Fontan completion, as well as survivors of less than five years duration because we aimed to evaluate precisely the clinical features of "well selected" atrial isomerism patients after successful establishment of the Fontan circulation.

We included the patients who had an IVC absence with azygos continuation and who underwent the Kawashima operation, which was historically positioned as a kind of definitive UVR at one short period. Their following clinical course was sometimes not satisfied because of oxygen desaturation associated with the development of PAVMs.²⁰ Although the pathogenesis of PAVMs was still considered multifactorial, it is not doubtful that the exclusion of hepatic venous blood containing some putative substance from the pulmonary circulation contributes to this occurrence.^{20,21} Hence, the converting to an EC-TCPC is sometimes useful to solve this problem.^{21,22} At present, we acknowledge the role of the Kawashima operation as a staging palliation aiming for EC-TCPC.

The mortality at the palliative operation and the Fontan-type operation was relatively higher than that reported in previous studies, because our series included a number of patients before the 1990s. For the same reason, the patient age at the time of the Fontan-type operation tended to be older, according to historical criteria.²³ Actually, the mean age at Fontan-type operation in our institution has been shifted from 9.8 ± 4.0 years old until the early 1990s to 3.0 ± 0.9 years old for the past decade. This strategic change may also play an optimal role to improve the survival of these patients.²⁴

CONCLUSIONS

Our analysis of the long-term survivors showed that there are still life-threatening problems 10 years after UVR. However, the excellent performance status of

the present long-term survivors suggests that these problems can all be overcome by the present strategies that have been established for the Fontan-type operation.

REFERENCES

1. Driscoll DJ, Offord KP, Feldt RH, et al: Five- to fifteen-year follow-up after Fontan operation. *Circulation* 1992;85:469-496.
2. Hashmi A, Abu-Sulaiman R, McCrindle BW, et al: Management and outcomes of right atrial isomerism: A 26-year experience. *J Am Coll Cardiol* 1998;31:1120-1126.
3. Gilljam T, McCrindle BW, Smallhorn JF, et al: Outcomes of left atrial isomerism over a 28-year period at a single institution. *J Am Coll Cardiol* 2000;36:908-916.
4. Cheung YF, Cheng VY, Chau AK, et al: Outcome of infants with right atrial isomerism: Is prognosis better with normal pulmonary venous drainage? *Heart* 2002;87:146-152.
5. Azakie A, Merklinger SL, Williams WG, et al: Improving outcomes of the Fontan operation in children with atrial isomerism and heterotaxy syndromes. *Ann Thorac Surg* 2001;72:1636-1640.
6. Stamm C, Friehs I, Duebener LF, et al: Improving results of the modified Fontan operation in patients with heterotaxy syndrome. *Ann Thorac Surg* 2002;74:1967-1977.
7. Yun TJ, Al-Radi OO, Adatia I, et al: Contemporary management of right atrial isomerism: Effect of evolving therapeutic strategies. *J Thorac Cardiovasc Surg* 2006;131:1108-1113.
8. Uemura H, Ho SY, Devine WA, et al: Atrial appendages and venoatrial connections in hearts from patients with visceral heterotaxy. *Ann Thorac Surg* 1995;60:561-569.
9. Kawashima Y, Kitamura S, Matsuda H, et al: Total cavopulmonary shunt operation in complex cardiac anomalies: A new operation. *J Thorac Cardiovasc Surg* 1984;87:74-81.
10. Gentles TL, Mayer JE Jr, Gauvreau K, et al: Fontan operation in five hundred consecutive patients: Factors influencing early and late outcome. *J Thorac Cardiovasc Surg* 1997;114:376-391.
11. Graham TP Jr, Johns JA: Pre-operative assessment of ventricular function in patients considered for Fontan procedure. *Herz* 1992;17:213-219.
12. Julsrud PR, Weigel TJ, Van Son JA, et al: Influence of ventricular morphology on outcome after the Fontan procedure. *Am J Cardiol* 2000;86:319-323.
13. McGuirk SP, Winlaw DS, Langley SM, et al: The impact of ventricular morphology on midterm outcome following completion total cavopulmonary connection. *Eur J Cardiothorac Surg* 2003;24:37-46.
14. Tanoue Y, Sese A, Ueno Y, et al: Bidirectional Glenn procedure improves the mechanical efficiency of a total cavopulmonary connection in high-risk Fontan candidates. *Circulation* 2001;103:2176-2180.
15. Laschinger JC, Redmond JM, Cameron DE, et al: Intermediate results of the extracardiac Fontan procedure. *Ann Thorac Surg* 1996;62:1261-1267.
16. Hsia TY, Migliavacca F, Pittaccio S, et al: Computational fluid dynamic study of flow optimization in realistic models of the total cavopulmonary connections. *J Surg Res* 2004;116:305-313.
17. Wu MH, Wang JK, Lin JL, et al: Supraventricular tachycardia in patients with right atrial isomerism. *J Am Coll Cardiol* 1998;32:773-779.
18. Dickinson DF, Wilkinson JL, Anderson KR, et al: The cardiac conduction system in situs ambiguous. *Circulation* 1979;59:879-885.
19. d'Udekem Y, Iyengar AJ, Cochrane AD, et al: The Fontan procedure: Contemporary techniques have improved long-term outcomes. *Circulation* 2007;116:1157-1164.
20. Stumper O, Wright JG, Sadiq M, et al: Late systemic desaturation after total cavopulmonary shunt operations. *Br Heart J* 1995;74:282-286.
21. McElhinney DB, Kreutzer J, Lang P, et al: Incorporation of the hepatic veins into the cavopulmonary circulation in patients with heterotaxy and pulmonary arteriovenous malformations after a Kawashima procedure. *Ann Thorac Surg* 2005;80:1597-1603.
22. Ichikawa H, Fukushima N, Ono M, et al: Resolution of pulmonary arteriovenous fistula by redirection of hepatic venous blood. *Ann Thorac Surg* 2004;77:1825-1827.
23. Choussat A, Fontan F, Besse P: Selection criteria for Fontan's procedure. In Anderson RH, Shinebourne EA, (eds): *Pediatric Cardiology*. Churchill Livingstone, Edinburgh, 1978, pp. 559-566.
24. Pearl JM, Laks H, Drinkwater DC, et al: Modified Fontan procedure in patients less than 4 years of age. *Circulation* 1992;86:1100-1105.

Adipose Tissue-Derived Multi-lineage Progenitor Cells as a Promising Tool for *In Situ* Stem Cell Therapy

Hanayuki Okura¹, Ayami Saga¹, Mayumi Soeda¹, Akihiro Ichinose² and Akifumi Matsuyama^{1,3,*}

¹Department of Somatic Stem Cell Therapy and Health Policy, Foundation for Biomedical Research and Innovation, 2-2 Minatojima-minamimachi, Chuo-ku, Kobe, 650-0047, Japan

²Department of Plastic Surgery, Kobe University Hospital, 7-5-2 Kusunoki-cho, Chuo-ku, Kobe, Hyogo, 650-0017, Japan

³The Center for Medical Engineering and Informatics, Osaka University, 2-2 Yamada-oka, Suita, Osaka, 565-0871, Japan

Abstract: Adipose tissue-derived cell sources are attractive for regenerative medicine due to the easy and safe accessibility of adipose tissue, lack of ethical issues, and their availability in large quantities. We have developed an isolation method for distinct stem cells, and named the cells adipose tissue-derived multilineage progenitor cells (ADMPC). ADMPC have higher potential for differentiation into adipocytic, osteocytic, and chondrocytic progeny than the widely reported adipose tissue-derived stromal/stem cells (ADSC). ADMPC can also differentiate into hepatocyte-like clusters *in vitro* by induction with the hepatogenic cytokines, hepatocyte growth factor, oncostatin M, and basic fibroblast growth factor. *In vivo*, ADMPC were reprogrammed *in situ* into hepatocyte-like cells that corrected the metabolic defect in hyperlipidemic Watanabe rabbits after transplantation *via* the portal vein. Such cells are potentially useful in regenerative medicine as sources for *in situ* stem cell therapy.

Keywords: adipose tissue, ADMPC, *in situ* stem cell therapy, *in situ* reprogramming, *in situ* differentiation, ADSC, ADMSC, ASC.

1. INTRODUCTION

The recent finding of differentiation-capable adult somatic stem cells holds great promise for regenerative medicine [1]. Extensive research is also ongoing into mesenchymal stem cells (MSC), found in human bone marrow, scalp tissue, placenta, umbilical cord matrix, and various fetal tissues [2-6]. Among these MSC sources, adipose tissue is particularly attractive for regenerative medicine because the tissues can be easily and safely accessed, are free of any ethical issues, and are available in large amounts. Many investigators have also reported that the cells derived from adipose tissue (adipose tissue-derived stromal/stem cells [ADSC], also referred to as adipose tissue-derived mesenchymal stem cells [ADMSC]) could differentiate into various cell types *in vitro* including chondrocytes, osteoblasts, adipocytes, myocytes, neuronal cells, and hepatocytes [1-4]. ADSC are considered as a colony-forming cell-rich fraction of adherent cells, which can attach to plastic culture dishes after isolation of the stromal vascular fraction (SVF), and thereafter be expanded and maintained in monolayer cultures as a heterogeneous population [7]. However, although ADSC can differentiate into various cell types *in vitro*, their self-renewal potency decreases significantly with passaging making them unsuitable for regenerative medicine applications.

In this review, we describe a novel population of adipose tissue-derived stem cells with higher differentiation potential than other well-reported adipose tissue-derived cells; we named these adipose tissue-derived multi-lineage progenitor cells (ADMPC). ADMPC could differentiate into hepatocyte-like cells *in vitro*, and in the hepatic environment *in vivo*. These *in situ* reprogrammed cells successfully corrected the metabolic defect in diseased animals, indicating that such *in situ* reprogramming could be applied for regenerative medicine as “*in situ* stem cell therapy”.

2. MATERIALS AND METHODS

2.1. Adipose Tissues

Adipose tissues were resected from five human subjects as excess discards during plastic surgery (females, age, 20-60 years). Ten to fifty grams of subcutaneous adipose tissue were collected from each subject. All subjects provided informed consent and the Review Board for Human Research of Kobe University Graduate School of Medicine and Foundation for Biomedical Research and Innovation approved the study protocol.

2.2. Isolation of ADMPC

Human ADMPC (hADMPC) were prepared as described previously [8-13]. Briefly, the resected adipose tissue was minced and then digested at 37°C for 1 h in Hank's balanced salt solution (HBSS, GIBCO Invitrogen, Grand Island, NY) containing 0.075% collagenase type II (Sigma Aldrich, St. Louis, MO). Digests were filtered through a cell strainer (BD Bioscience, San Jose, CA) and centrifuged at 800 x g for 10

*Address correspondence to this author at the Department of Somatic Stem Cell Therapy and Health Policy, Foundation for Biomedical Research and Innovation, 2-2 Minatojima-minamimachi, Chuo-ku, Kobe, 650-0047, Japan; Tel: +81-78-304-8706; Fax: +81-78-304-8707; E-mail: akifumi-matsuyama@umin.ac.jp

min. Red blood cells were excluded using density gradient centrifugation with Lymphoprep ($d = 1.077$; Nacalai Tesque, Kyoto, Japan), and the remaining cells were cultured in Dulbecco's modified Eagle's medium (DMEM, GIBCO Invitrogen) with 10% defined fetal bovine serum (FBS, GIBCO Invitrogen) for 24 h at 37°C. Following incubation, the adherent cells were washed extensively and then treated with 0.2 g/l ethylenediaminetetraacetate (EDTA) solution (Nacalai Tesque). The resulting suspended cells were replated at a density of 10,000 cells/cm² on human fibronectin (FN)-coated dishes (AGC, Tokyo, Japan) in Stem Cell Medium (Nipro, Osaka, Japan) containing 1 x insulin-transferrin selenium (ITS, GIBCO Invitrogen.), 1 nM dexamethasone (Sigma Aldrich), 100 μM ascorbic acid 2-phosphate (Sigma Aldrich), 10 ng/ml epidermal growth factor (EGF, PeproTec, Rocky Hill, NJ), and 5% FBS. After passaging 5 to 6 times in the same medium, the ADMPC were ready for use in experiments. ADSC were isolated and cultured as reported by Zuk *et al.* [7].

2.3. Adipocytic, Osteocytic, and Chondrocytic Differentiation Procedure

For adipocytic differentiation, cells were cultured in Differentiation Medium (Zen-Bio, Research Triangle Park, NC) [14]. After three days, half of the medium was replaced with Adipocyte Medium (Zen-Bio) and this was repeated every two days. Five days after differentiation, adipocytes were identified by intracellular lipid droplets observed microscopically after Oil Red O staining. In brief, cultures were fixed in Baker's formal calcium, washed in 60% isopropanol, and stained with double-filtered Oil Red O solution to identify lipid accumulation. To determine the lipid content, Oil-Red O was extracted from the differentiated cells with isopropanol and absorbance of the contents was evaluated. Osteocytic differentiation was induced by culturing the cells in DMEM containing 10 nM dexamethasone, 50 mg/dl ascorbic acid 2-phosphate, 10 mM beta-glycerophosphate (Sigma Aldrich), and 10% FBS. Differentiation was evaluated by Alizarin red staining and alkaline phosphatase (ALPase) activity as described previously [15]. For Alizarin red staining, the cells were washed three times and fixed with dehydrated ethanol. After fixation, the cells were stained with 1% Alizarin red S in 0.1% NH₄OH (pH 6.5) for 5 minutes, and then washed with H₂O. ALPase activity per cell was calculated based on the amount of DNA. For chondrocytic differentiation, ADMPC were trypsinized and 2 x 10⁵ cells were centrifuged at 400 x g for 10 minutes. The resulting pellets were cultured in chondrogenic medium (α -MEM supplemented with 10 ng/ml transforming growth factor (TGF)- β , 10 nM dexamethasone, 100 μM ascorbate, and 10 μg/ml 100 x ITS Solution) for 14 days [8]. The osteogenic differentiation was assessed by Alcian Blue staining, whereby nuclear counterstaining with Weigert's hematoxylin was followed by 0.5% Alcian Blue 8GX, which binds proteoglycan-rich cartilage matrix.

2.4. Differentiation of Hepatocyte-Like Cell Clusters

The differentiation procedure consisted of three stages. In stage I, ADMSC were cultured and expanded in medium I for three to four passages. In stage II, the cells were dissociated with trypsin-EDTA and the resulting single cells were suspended in medium II (80% knockout-DMEM [GIBCO

Invitrogen], 20% defined FBS, 1 mM glutamine, and 1% nonessential amino acids [both from GIBCO Invitrogen]). The suspension was placed in an ultralow-attachment culture dish (Hydrocell; CellSeed, Tokyo, Japan), and the cells self-aggregated into cell clusters within 1 day. The cell clusters were then cultured for an additional 2 days. In stage III, after washing extensively with PBS, 2-day-old cell clusters (average of 1000 cells each) were cultured on a Hydrocell dish for 4 weeks in medium III (60% DMEM-low glucose, 40% MCDB-201, 1 nM dexamethasone, 100 mM ascorbic acid, 10 ng/ml EGF, basic fibroblast growth factor [bFGF, Peprotech, Rocky Hill, NJ], hepatocyte growth factor [HGF, Peprotech], and oncostatin M [OSM]). Finally, 0.1% dimethyl sulfoxide (DMSO; Nacalai Tesque) was added on the 10th day after induction of differentiation.

2.5. DiO or DiI Labeling of LDL

Human LDL (density 1.019-1.063 g/ml) was isolated by sequential ultracentrifugation from normolipidemic donors, dialyzed against saline-EDTA, and then sterilized by filtration through a 0.2-μm filter. Lipoproteins were labeled with DiO or DiI (Sigma) by incubating the LDL in 0.5% bovine serum albumin (BSA)/PBS with 100 ml DiO or DiI in DMSO (3 mg/ml) for 8 h at 37°C. The lipoproteins were then dialyzed against PBS and filtered before use.

2.6. Cell Transplantation and Immunosuppression

The protocols for cell transplantation and immunosuppression were described previously [12]. In brief, WHHL rabbits (8-week-old, purchased from Kitayamalabes, Ina, Nagano, Japan) were anesthetized with 50 mg/kg pentobarbital. An incision distal and parallel to the lower end of the ribcage was made, followed by a peritoneal incision and infusion of the ADMPC or control into the portal vein. The immunosuppression regimen consisted of the following: i) intramuscular injection of 6 mg/kg/day cyclosporin A daily from the day before surgery to sacrifice, ii) intramuscular injection of 0.05 mg/kg/day rapamycin daily from the day before surgery to sacrifice, iii) methylprednisolone at 3 mg/kg/day (day -1 to 7), followed by tapering to 2 mg/kg/day (day 8 to 14), 1 mg/kg/day (day 15 to 21), and 0.5 mg/kg/day (day 22 to the time at sacrifice), iv) intravenous injection of 20 mg/kg/day cyclophosphamide at days 0, 2, 5, and 7, and v) intramuscular injection of 2.5 mg/kg/day ganciclovir to avoid viral infection in the immunocompromised host.

2.7. Immunohistochemical Staining of WHHL Rabbit Liver Sections

The WHHL livers were harvested and fixed immediately with 10% formalin. They were placed into optimal cutting temperature (OCT) compound (Sakura Finetechnical), frozen immediately, and then sectioned at 7 μm-thickness. The sections were incubated with blocking solution (Blocking one; Nacalai Tesque) for 1 h, and then incubated with rabbit anti-human albumin antibody (MBL, Nagoya, Japan) or mouse anti-human CD90 antibody followed by Alexa Fluor 488-labeled goat anti-rabbit IgG or Alexa Fluor 546-labeled goat anti-mouse IgG (Molecular Probes, Eugene, OR). The stained sections were examined with a BioZero laser scanning microscope (Keyence, Osaka, Japan).

Table 1. Differences Between ADMPC and ADSC of their Differentiation / Proliferation Abilities

	Self-Aggregation Properties	EDTA-Sensitiveness	Differentiation Abilities			Proliferation Abilities	
			Adipocytic	Osteocytic	Chondrocytic	After Reseeding	After β Passaging
ADMPC	+	+	++	++	++	+	++
ADSC	-	-	+	+	+	++	++

2.8. PCR Analysis of WHHL Rabbit Liver for Human Liver-Specific Genes

Total RNAs of WHHL rabbit liver, hADMPC, and human hepatocytes were isolated using an RNAeasy kit (Qiagen, Valencia, CA). After treatment with DNase, the cDNAs were synthesized using Superscript III RNase H-minus Reverse Transcriptase (Invitrogen). Real-time PCR was performed using the ABI Prism 7900 Sequence Detection System (Applied Biosystems, Foster City, CA). 20X Assays-on-Demand™ Gene Expression Assay Mix for human alpha-1-antitrypsin (hAAT1) (Hs01097800_m1), human albumin (Hs00609411_m1), human Factor 9, human GATA4 (Hs00171403_m1), human hepatocyte nuclear factor 3beta (HNF-3beta) (Hs00232764_m1), human LDL receptor (Hs00181192_m1), and human glyceraldehyde-3-phosphate dehydrogenase (GAPDH) (Hs99999905_m1) were obtained from Applied Biosystems. It was confirmed that our human detectors and rabbit detectors did not cross-react with the other species. TaqMan® Universal PCR Master Mix and No AmpErase® UNG (2X) were also purchased from Applied Biosystems. Reactions were performed in quadruplicate and the mRNA levels were normalized relative to human GAPDH expression. To confirm that hADMPC differentiated into hepatocytes *in vivo*, the cells were tested by quantitative PCR before transplantation using human primary hepatocytes (Invitrogen, Lot number; HuP81) as controls.

2.9. Assay for Lipid Profiling

Serum samples were obtained from nonfasting rabbits before and after transplantation. Serum total cholesterol was measured in each sample using assay kits from Wako Pure Chemical Industries (Osaka, Japan). Serum lipoproteins were analyzed by an on-line dual enzymatic method for simultaneous quantification of cholesterol and triglycerides by high-performance liquid chromatography at Skylight Biotech (Akita, Japan), according to the described procedure [21].

2.10. Clearance of 125 I-LDL from Rabbit Serum

WHHL rabbits (8 weeks old) were anesthetized with pentobarbital (50 mg/kg). The peritoneum was incised and hADMPC (high-dose; 3×10^7 cells/rabbit, $n = 2$, low-dose; 5×10^6 cells/rabbit, $n = 2$) suspended in 3 ml of HBSS (20°C) ($n = 5$) or 3 ml of control ($n = 2$) were infused into the portal vein via an 18-gauge Angiocath™ (BD, UT). Eight weeks later, the animals were tested by the LDL turnover assay. 125 I-labeled human LDL (BT-913R, Biomedical Technologies, Stoughton, MA) was delivered via the marginal ear vein of the WHHL rabbits. Blood was collected from the opposite ear after injection at 5 min, 1 h, 2 h, 4 h, 6 h, and 28

h. 125 I-labeled apolipoprotein B-containing LDL was precipitated with 20% trichloroacetic acid (Wako Pure Chemical Industries) (serum; 320 μ l, 100% w/v TCA 80 μ l), and then the precipitants were applied for counting.

2.11. Statistical Analysis and Ethical Considerations

All animal studies described in this report were approved by Kobe University Graduate School of Medicine and Foundation for Biomedical Research and Innovation. Values were expressed as mean \pm SEM. Differences between mean values of treated and untreated groups were evaluated using the Student's t-test. A P value less than 0.05 was considered statistically significant. All statistical analyses were performed using the SPSS Statistics 17.0 package (SPSS Inc., Chicago, IL).

3. RESULTS AND DISCUSSION

3.1. Self-Aggregation Properties and EDTA-Sensitivity of ADMPC

In the ADMPC isolation procedure were shown in Fig. (1A) (cited from reference 12 with modification). First, we removed contaminating red blood cells using density gradient centrifugation after digestion of adipose tissue to obtain the stromal vascular fraction (SVF). After 24-hour culture of the SVF (Fig. 1Aa), adherent cells were treated with EDTA solution and the suspended cells were collected. Finally, these cells were re-plated on human FN-coated dishes (Fig. 1Ab) and cultured (Fig. 1Ac). Within 2–3 passages after the initial plating of the primary culture, ADMPC appeared as a monolayer of large flat cells (25–30 μ m in diameter). As the cells approached confluence, they became spindle-shaped, resembling fibroblasts (Fig. 1Ad). We next analyzed the mRNA expression levels of *islet-1* and *nkx2.5* in the two types of cells. *Islet-1* is a marker of undifferentiated cells and progenitors of cardiomyocytes, hepatocytes and pancreatic β cells, and *nkx2.5* is a marker of progenitors of cardiomyocytes. As shown in Fig. (1B), *islet-1* and *nkx2.5* were expressed in ADMPC, but not in ADSC. No or faint staining was noted for *GATA-4*, *myosin light chain*, *alpha cardiac actin*, and *myosin heavy chain* expression in both ADMPC and ADSC. On the other hand, flowcytometric analysis showed no significant different pattern in their cell surface markers between ADMPC and ADSC.

3.2. Adipocytic, Osteocytic and Chondrocytic Differentiation

In the next step, we assessed whether the adipocytic, osteocytic, and chondrocytic differentiation potentials of ADMPC were higher than those of ADSC (Table 1). Adipo-

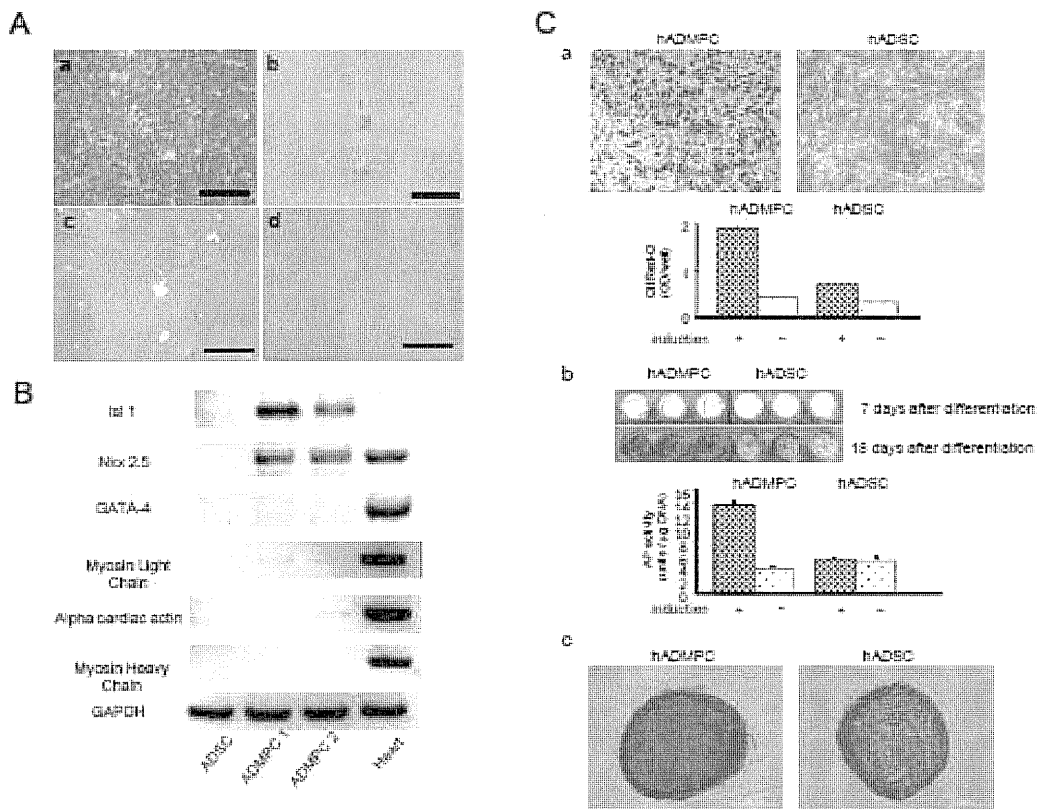


Fig. (1). Characters of ADMPC. (A) Morphological characteristics of ADMPC. The cells obtained from adipose tissue were seeded and incubated for 24 h (a). Following incubation, the adherent cells were treated with EDTA solution, and the resulting suspended cells were replated at a density of 10,000 cells/cm² on human fibronectin (FN)-coated dishes (BD BioCoat) (b and c). Within 2–3 passages after the initial plating of the primary culture, ADMPC appeared as a monolayer of large flat cells (25–30 μ m in diameter). As the cells approached confluence, they assumed a more spindle-shaped, fibroblastic morphology (d). Calibration bars = 500 μ m (a, c and d) and 200 μ m (b). Cited from reference 12 with modification. (B) Comparison of mRNA expression of markers of undifferentiated cells on ADMPC and ADSC. Islet-1, a marker of undifferentiated cells and progenitors of cardiomyocytes, hepatocytes, and pancreatic β cells, and nkx2.5, a transcription factor known to mark cardiomyocyte differentiation, were expressed in ADMPC, but not ADSC. GATA-4, a myosin light chain protein, α -cardiac actin, and myosin heavy chain protein were absent or only faintly stained in both cell types. Human heart mRNA was used as the control in these experiments. (C) Differences in the differentiation potentials between ADMPC and ADSC. (a) Morphological comparison of the adipogenic differentiation potential of ADMPC and ADSC. The cells were cultured in Differentiation Medium. After three days, half of the medium was replaced with adipocyte medium and this was repeated every two days. Five days after differentiation, the lipid contents of differentiated adipocytes were confirmed by Oil Red O staining. The lipid contents of differentiated adipocytes were confirmed by Oil Red O extraction. hADMPC showed higher lipid contents than hADSC. Data are mean \pm SEM of triplicate experiments. (b) Morphological comparison of osteogenic differentiation potential of ADMPC and ADSC. At 7 or 18 days after osteogenic differentiation, the cells were stained with Alizarin red S for mineralized nodules. ADMPC showed higher osteogenic differentiation potential than ADSC. even days after osteogenic differentiation, the cells were assayed for alkaline phosphatase (APase) activity. AP activity per cell was calculated based on the amount of DNA. hADMPC showed higher APase activity than hADSC. Data are mean \pm SEM of triplicate experiments. (c) Comparison of chondrogenic differentiation potential between ADMPC and ADSC. Extracellular matrices of differentiated ADMPC and ADSC into chondrocytes were visualized with Alcian Blue staining.

cytic differentiation was induced by culture with the Differentiation Medium containing 1-methyl-3-isobutylxanthine, dexamethasone, and insulin. Induction was confirmed by the accumulation of intracellular lipid droplets that could be stained with Oil Red O. The results showed higher levels of adipocytic induction for ADMPC than ADSC (Fig. 1Ca). Next, osteocytic induction was examined by Alizarin red S staining (Fig. 1Cb). After a 7-day induction for osteocytic differentiation, ADMPC only were stained with Alizarin red S. ADSC were stained after an 18-day induction, but their staining intensity lagged behind that of ADMPC (Fig. 1Cb). Third, the chondrocytic differentiation potential of ADMPC and ADSC was compared. As shown in Fig. (1Cc), ADMPC

showed more intense Alcian Blue staining than ADSC, suggesting higher chondrocytic induction for ADMPC than ADSC. The self-aggregation properties of ADMPC might introduce their higher chondrocytic induction than ADSC. These results indicated that ADMPC have higher differentiation potentials than ADSC.

3.3. *In Vitro* Differentiation of ADMPC into Hepatocytes

To obtain hepatocyte-like cell clusters, we have established a three-step method (Fig. 2A). Immunofluorescence staining (Fig. 2B) showed albumin- and alpha-1-antitrypsin-expressing cells among the differentiated ADMPC (cited from reference 10 with modification). The ability to secrete

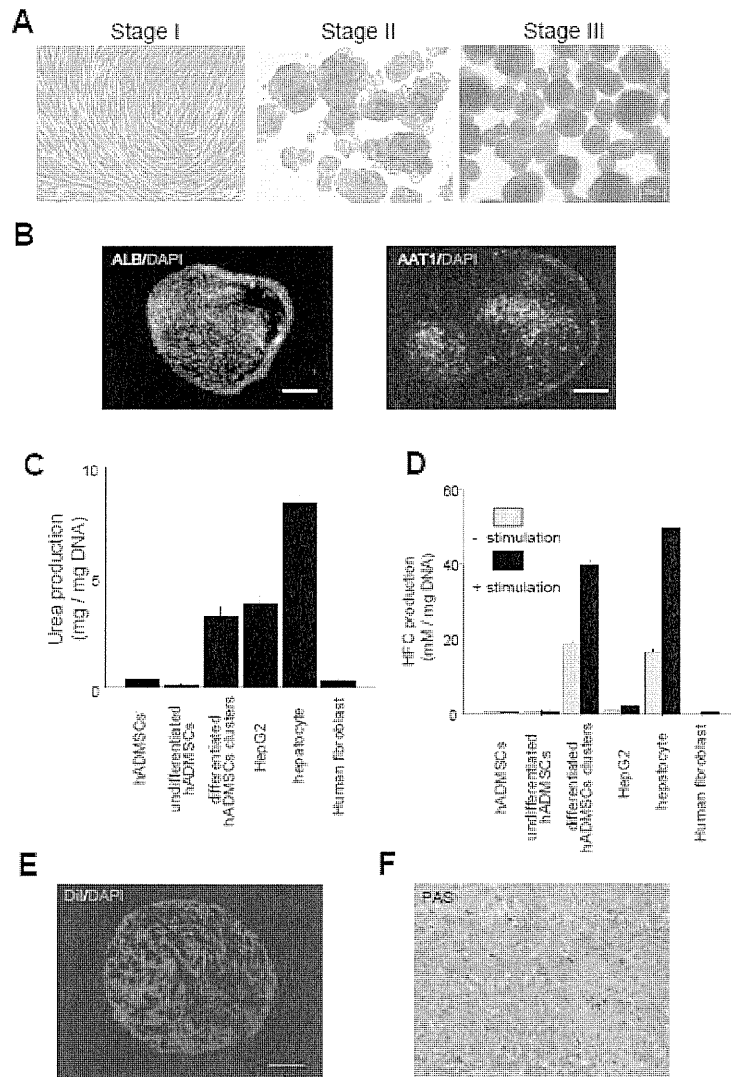


Fig (2). (A) General outline of the three-stage differentiation protocol. Stage I: growth of hADMPCs. Stage II: formation of cell clusters by culture in low osmotic medium on ultralow-attachment culture dishes. Stage III: growth factor stimulation of cell cluster cultures with bFGF, HGF, and OSM. DMSO was added on the 10th day after induction. (B) Immunofluorescence staining for ALB (left) and AAT (right) in differentiated ADMPC clusters. Scale bar, 100 μ m. (C) Urea synthesis by differentiated ADMPC clusters after incubation with 5 mM NH_4Cl . Urea synthesis per cell was calculated based on the amount of DNA. Data are mean \pm SEM of triplicate experiments. (D) CYP enzyme activity in differentiated ADMPC clusters, as determined by hydroxylation of 7-benzyloxy-4-trifluoromethoxy-coumarin to HFC. Before incubation with 100 mM, cells were cultured in the absence (non-stimulation) or presence (stimulation) of 10 mM rifampicin. CYP activity per cell was calculated based on the amount of DNA. Data are mean \pm SEM of triplicate experiments. (E) Low-density lipoprotein uptake by differentiated ADMPC clusters. Samples were examined by confocal laser scanning microscopy. Scale bar, 100 μ m. (F) Glycogen storage in differentiated ADMPC clusters, as determined by PAS staining. hALB, human ALB; SEM, standard error of the mean; HFC, 7-hydroxy-4-trifluoromethyl-coumarin; PAS, periodic acid-Schiff's; DiI, 1,10-dioctadecyl-3,3',30,30'-tetramethylindocarbocyanine; DAPI, 4,6-diamidino-2-phenylindole.

urea was about 12-fold higher for differentiated ADMPC incubated with NH_4Cl , compared with stage I undifferentiated ADMPC, and as high as that of HepG2 cells (Fig. 2C). Nonfluorescent 7-benzyl-trifluoromethyl coumarin (BFC) is metabolized mainly by the cytochrome P450 (CYP) 3A family of enzymes and converted to the fluorescent 7-hydroxy-4-trifluoromethylcoumarin (HFC). The concentration of HFC in the supernatant was measured after incubation with 100 mM BFC. CYP activity in differentiated ADMPC clusters was 40-fold higher than in undifferentiated ADMPC (Fig. 2D). In addition, CYP activity in differentiated ADMPC clusters increased 2–2.5-fold following preincubation with

rifampicin for 3 days. In contrast, no increase in CYP activity was induced in undifferentiated ADMPC under this condition. We also assessed LDL uptake by differentiated ADMPC clusters by incubating differentiated ADMPC with DiI-LDL (Fig. 2E). DiI-LDL was markedly incorporated into the cytosol of differentiated ADMPC. Another function of hepatocytes is glycogen production (glyconeogenesis), and PAS staining showed glycogen storage in differentiated ADMPC (Fig. 2F). These results suggest that hepatogenic cytokines and floating culture could mimic the liver micro-environment and promote the differentiation of ADMPC into hepatocyte-like cells *in vitro*.

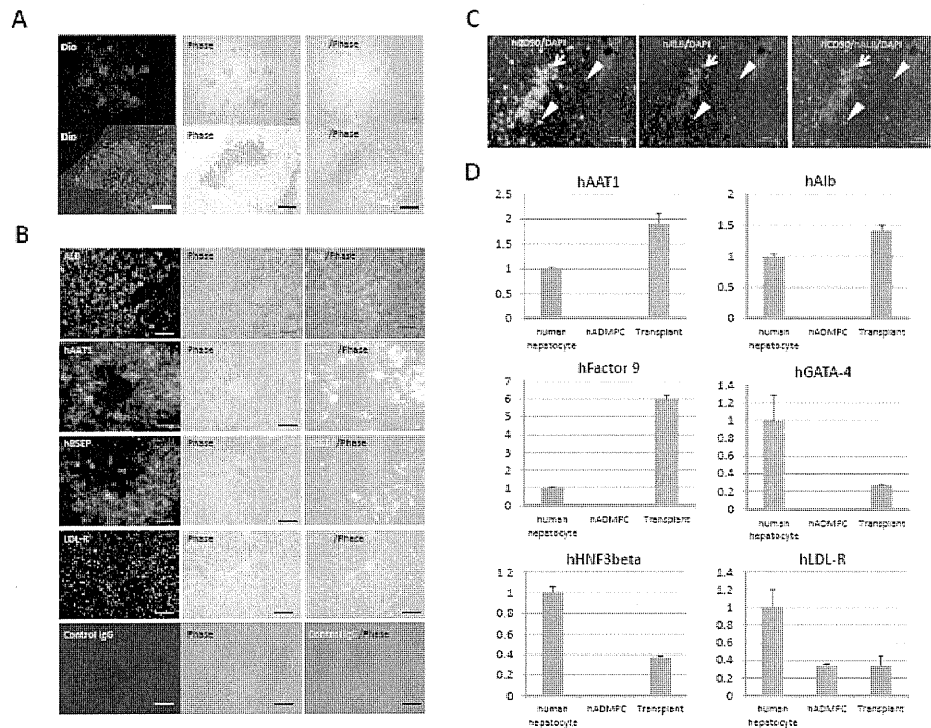


Fig (3). (A) Localization of transplanted hADMPCs in the WHHL liver. One week after transplantation of DiO-labeled hADMPCs via the portal vein, the WHHL rabbit liver was examined histologically. The DiO-labeled cells were localized in the portal area and dispersed in a centrilobular direction, resembling the mature innate hepatocytes. Bars = 200 μ m (upper panels) and 100 μ m (lower panels). (B) Immunohistochemical identification of human hepatocytic marker cells in liver sections of WHHL rabbits after ADMPC transplantation. Twelve weeks after ADMPC transplantation, human albumin-, human alpha-1-antitrypsin-, human bile salt export pump (BSEP)-, and LDL-receptor-positive cells were dispersed within the peri-venous regions of the liver parenchyma, where they made contact with and integrated among the host cells with cell-cell interactions between ADMPC-derived cells and diseased hepatocytes. Bar = 100 μ m. (C) Differentiation of transplanted ADMPC into hepatocyte-like cells. Twelve weeks after transplantation, nearly all the human CD90-positive cells expressed human albumin, indicating that the major proportion of transplanted ADMPC could differentiate into hepatocyte-like cells (left panel: human CD90; middle panel: human albumin; right panel: merge). Arrows indicate human CD90 and human albumin double-positive cells; arrowheads indicate human CD90-positive/human albumin-negative cells. (D) Human hepatic gene expression in WHHL rabbit liver after ADMPC transplantation. RNA was prepared from WHHL rabbit livers 12 weeks after ADMPC transplantation. We examined expressions of the following hepatic markers by quantitative real time-polymerase chain reaction (RT-PCR) using the Assays-on-Demand Gene Expression Assay Mix: human alpha-1-antitrypsin, human albumin, human factor IX, human GATA-binding protein 4 (GATA-4), human hepatocyte nuclear factor 3 (HNF-3) beta, and human LDL-receptor. The livers of the control WHHL rabbits (saline, n = 3) were negative for all tested human hepatic genes. The mRNA levels were normalized based on human glyceraldehyde-3-phosphate dehydrogenase as a housekeeping gene and data are expressed as mean \pm SEM of triplicate experiments. The livers of ADMPC-recipient WHHL rabbits (n = 3) were positive for all tested human hepatic genes, which showed expression levels similar to those of human primary hepatocytes, but not ADMPC *per se*. Data are mean \pm SEM.

3.4. *in situ* Reprogramming of ADMPC into Hepatocytes

One week after transplantation of hADMPC via the portal vein, we examined whether the cells reside or not in the liver after transplantation. As shown in Fig. (3A), DiO-fluorescent labeled-hADMPC resided and distributed in the portal area, and morphologically resembled innate hepatocytes. Next, we should examine the recruitment of these cells directly into the rabbit liver and the success of hepatocytic differentiation. For this purpose, we measured human-specific hepatocytic proteins and their hepatic functions (Fig. 3, cited from reference 12 with modification). Human albumin-, alpha-1-antitrypsin-, bile salt export pump-, and LDL-receptor-positive cells were dispersed within peri-venous regions of the liver parenchyma, where they had contacted and integrated among the host cells (Fig. 3B). We also identified conserved cell-cell interactions between ADMPC-derived and diseased hepatocytes. To confirm this finding

and to assess the efficacy of differentiation, we colocalized human CD90 and human albumin. As shown in Fig. (3C), nearly all human CD90-positive cells expressed human albumin, indicating that about 80% or more of transplanted ADMPC differentiated into human albumin-positive hepatocyte-like cells at 12 weeks after transplantation. Next, to confirm the differentiation of ADMPC into hepatocytes *in vivo*, the expression of hepatocyte markers was analyzed by quantitative RT-PCR. WHHL rabbit liver that was transplanted with ADMPC expressed higher levels of human-specific alpha-1-antitrypsin, albumin, and coagulation factor IX than control ADMPC (Fig. 3D). The expression levels of human GATA-4, human hepatocyte nuclear factor 3 beta, and LDL-receptor were also higher in the WHHL rabbit liver than in the ADMPC untransplanted liver (Fig. 3D). These results verified that ADMPC *per se* could differentiate into mature hepatocytes *in vivo*.

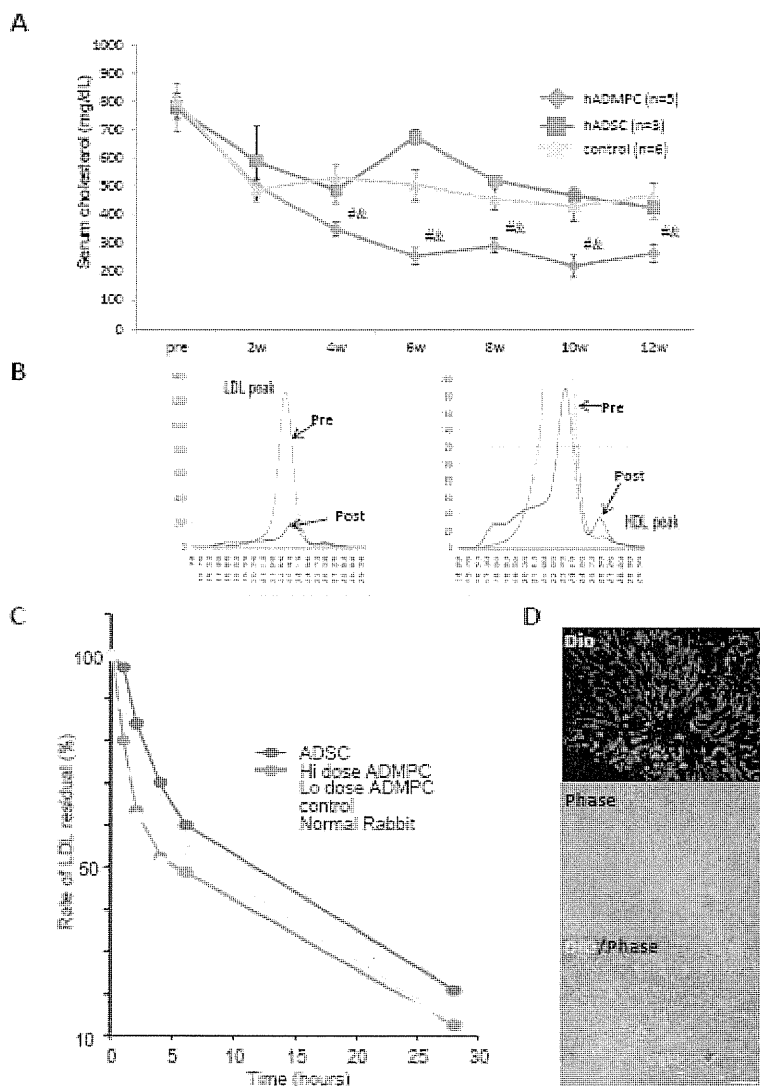


Fig. (4). (A) Total serum cholesterol levels. ADMPC transplantation in WHHL rabbits was followed for 12 weeks. Total serum cholesterol was measured in five rabbits that each received 3×10^7 ADMPC, three rabbits that each received 3×10^7 ADSC, and in six rabbits that received saline (control). Data are mean \pm SEM. $\#P < 0.05$; control vs. the ADMPC-transplanted WHHL rabbit; $\&P < 0.05$; the ADSC-transplanted WHHL rabbit vs. the ADMPC-transplanted WHHL rabbit). (B) Lipoprotein profiles in a representative WHHL rabbit with ADMP transplantation after gel filtration. Serum samples from the WHHL rabbit before and 4 weeks after transplantation were fractionated. Note the marked reduction in low-density lipoprotein (LDL) peak and appearance of a high-density lipoprotein (HDL) peak. (C) Rate of clearance of LDL from the serum of rabbits with and without transplantation of ADMPC. Animals were injected with ^{125}I -labeled human LDL, and the time course of clearance was monitored following trichloroacetic acid precipitation of serum at 5 min, 1 h, 2 h, 4 h, 6 h, and 28 h. Residual ^{125}I -LDL was expressed as a percentage of the signal at 5 min. The panel is the representative of two independent experiments. (D) DiO-LDL uptake into ADMPC-derived hepatocytes in the WHHL rabbit liver. Thin slices of recipient liver were incubated with DiO-labeled LDL in the serum-free medium for 24 h. After washing and fixation, the incubated slices were viewed by fluorescence microscopy. DiO-LDL-uptake cells (green) and no-uptake parenchymal cells are observed in the section. Bar = 100 μm .

3.5. In Situ Stem Cell Therapy by ADMPC

To determine the effects of ADMPC transplantation on the recipient rabbit lipid profile, serum cholesterol levels were monitored over 12 weeks (Fig. 4, cited from reference 12 with modification). Significant reductions in total serum cholesterol were observed within 4 weeks of the transplantation, and the reductions were maintained for the entire period (Fig. 4A). Furthermore, ADMPC-recipient animals showed significantly greater reductions than those in the control group. To determine the effects of ADMPC transplantation on the fractions of high-density lipoprotein and LDL in re-

ipient animals, fractionation by fast protein liquid chromatography was performed (Fig. 4B). Transplantation of ADMPC resulted in marked reduction of the peak LDL cholesterol and increment of high-density lipoprotein cholesterol fraction (right panel). Next, clearance experiments were performed with human LDL to confirm that the transplanted ADMPC contributed to the fall in serum cholesterol through uptake of LDL via LDL receptors. The rate of LDL clearance was significantly higher in the WHHL rabbits with transplanted ADMPC than WHHL rabbits without transplanted ADMPC (Fig. 4C). Rabbits with ADMPC transplants showed ~ 2.4 -fold (high-dose; 3×10^7 cells/rabbit) and

1.4-fold (low-dose; 5×10^6 cells/rabbit) increases in the rate of LDL cholesterol clearance over non-transplanted rabbits. To evaluate the uptake of DiO-LDL by transplants *ex vivo*, thin liver slices of WHHL rabbit were incubated with DiO-labeled LDL for 24 h and the uptake was examined as for the clearance experiments (Fig. 4D). DiO-LDL was taken up by some but not all of the cells in the WHHL rabbit liver transplanted with ADMPC, with the positive cells observed dispersed, contacting, and integrating among the non DiO-LDL-positive parenchymal cells. This finding suggests that ADMPC differentiated into hepatocytes *in vivo*, thus lowering the serum cholesterol directly via LDL uptake.

3.6. ADMPC as a Promising Tool for Regenerative Medicine

For any successful regenerative medicine program, three issues must be considered: 1) what kind of tissues should be nominated as cell sources, 2) how should the cells be obtained from tissues, and 3) how will the cells behave after transplantation/administration. The following section discusses these considerations with respect to this study.

The source of stem cells for regenerative medicine should be easily and safely accessible as well as free of any ethical issues, thus allowing allogenic as well as autologous cellular therapy applications, and finally, the cell source should be available in large amounts. Adipose tissue is therefore a suitable cell source under these criteria. Liposuction surgery provides a safe method for collection of adipose tissue, harvesting from 100 ml to >3 L of lipoaspirate from material that is routinely discarded, thus avoiding any ethical concerns [16].

As to the second issue of cell processing, methods to isolate cells from adipose tissue were first reported in the 1960s [17-19]. Such methods involved mincing rat fat pads and incubating the resultant tissue fragments with collagenase. The digested material was then centrifuged to separate the floating population of mature adipocytes from the pelleted stromal vascular fraction (SVF). The SVF, which are sometimes referred to as adipose tissue-derived regenerative cells (ADRC), consists of a heterogeneous cell population including fibroblasts, endothelial cells, pre-adipocytes, and mesenchymal stem cells [17-19]. However, as mentioned, this non-cultured cell population is too heterogeneous to apply therapeutically, necessitating the isolation of pre-adipocyte and/or mesenchymal stem cell-rich adherent cells from the SVF. The original procedure for this separation step was subsequently modified for the isolation of cells from human adipose tissue SVFs [20-23], and Zuk *et al.* [7] reported that the processed lipoaspirates exhibited mesenchymal stem cell-like features and could differentiate into adipocytes, osteocytes, and chondrocytes. Such cells are currently labeled as adipose tissue-derived stem cells (ADSC). The procedure used for obtaining these stem cells from lipoaspirates was described by Bjornorp *et al.* [24] to obtain pre-adipocytes.

We have subsequently developed a novel isolation method for stem-like cells according to their adhesion properties [8-12]. As shown in Fig. (1Aa), fibroblast- and endothelial-like cells completely adhered onto the culture dish after 24 h in culture following the first-plating of the SVF. Most of the SVF cells were difficult to detach by conven-

tional pipetting after this length of culture (24 h). However, a population of round self-aggregating cells that could only be detached by treatment with EDTA solution showed multilineage differentiation potency. In the EDTA-treating method, only cells of their properties with self-aggregation and EDTA-sensitiveness could be selected as ADMPC from plated SVF. In the conventional pre-plating methods to obtain ADSC [7, 24], the cells with EDTA-resistance could not be excluded. ADMPC exhibited high differentiation capacities for osteocytic, adipocytic, and chondrocytic lineages compared with ADSC, and could differentiate into hepatocyte-like cells, insulin-producing cells, and cardiomyoblast-like cells *in vitro* as non-mesenchymal lineages. We therefore named these cells ADMPC.

ADMPC differ from ADSC with regard to gene expression profiling. ADMPC express islet-1, a marker of undifferentiated cells and of cardiac, hepatic, and pancreatic progenitor cells [9-11]. Based on our findings, we propose that the islet-1-expressing ADMPC could be differentiated or reprogrammed into hepatocytes in the recipient liver *in vivo* after transplantation. In other words, the appropriate cells can show *in situ reprogramming* when transplanted and recruited into an appropriate environment.

Finally, we considered how the ADMPC would behave after transplantation/administration *in situ*. Traditionally, stem/progenitor cells are differentiated into terminally differentiated cells prior to transplantation/administration. For example, iPS cells are differentiated into neuronal cells and then applied for neuronal disease therapies. In these processes, researchers could mimic the relevant microenvironment and then differentiate the transplanted cells into the desired cell lineages. In contrast, we hypothesized that *in vitro* or *ex vivo* reprogramming could not sufficiently recapitulate the desired transplant microenvironment. Our concept is that the microenvironment *in situ* might supply cytokines to exert paracrine effects and form appropriate extracellular matrices, thus prompting the progenitor cells toward the desired terminal differentiation. ADMPC express islet-1, indicating that they might be appropriate progenitor cells on their own for *in situ* reprogramming as hepatocytes in the liver microenvironment. If these reprogrammed cells could correct given disease defects, clinical applications for *in situ* stem cell therapy become feasible.

In this review, we propose *in situ* stem cell therapy as a new tool for regenerative medicine and *in situ* reprogramming as a mechanism for the correction of disease. Yamana *et al.* [25] presented terminally differentiated cells that could be reprogrammed into the pluripotent state using only four factors. Followers confirmed the fact and named the concept "reprogramming". Melton *et al.* [26] subsequently showed that gene-modified cells alone could direct differentiation along a terminal path, and renamed the mechanism "direct reprogramming", and some cases of *ex vivo* gene therapy might be included in this concept. Here, we presented stem-like cells that could differentiate terminally *in situ* in the appropriate microenvironment.

4. CONCLUSIONS

In this review we describe ADMPC, novel adipose tissue-derived cells with stem cell-like properties and higher

differentiation potential than previously reported adipose tissue-derived cells. Not only could ADMPC differentiate into hepatocyte-like cells *in vitro*, but ADMPC *per se* also showed the same capacity in the hepatic environment and the *in situ* reprogrammed cells could correct the metabolic defect of diseased animals. The mechanisms described for *in situ* reprogramming hold great promise for applications in regenerative medicine as “*in situ* stem cell therapy”.

ACKNOWLEDGMENTS

This study was supported in part by the Program for Promotion of Fundamental Studies in Health Sciences of the National Institute of Biomedical Innovation (NIBIO) and Kobe Translational Research Cluster, the Knowledge Cluster Initiative, Ministry of Education, Culture, Sports, Science and Technology (MEXT).

DISCLOSURE

It should be noted that the authors have previously published much of the material covered in this review article in “Tissue Eng Part C Methods”, Volume 17, 2011, Pages 145-154.

CONFLICT OF INTEREST

The authors declare no conflict of interest.

REFERENCES

- [1] Wagers AJ, Weissman IL. Plasticity of adult stem cells. *Cell* **2004**, 116, 639-648.
- [2] Pittenger MF, Mackay AM, Beck SC, Jaiswal RK, Douglas R, Mosca JD, Moorman MA, Simonetti DW, Craig S, Marshak DR. Multilineage potential of adult human mesenchymal stem cells. *Science* **1999**, 284, 143-147.
- [3] Shih DT, Lee DC, Chen SC, Tsai RY, Huang CT, Tsai CC, Shen EY, Chiu WT. Isolation and characterization of neurogenic mesenchymal stem cells in human scalp tissue. *Stem Cells* **2005**, 23, 1012-1020.
- [4] In 't Anker PS, Scherjon SA, Kleijburg-van der Keur C, de Groot-Swings GM, Claas FH, Fibbe WE, Kanhai HH. Isolation of mesenchymal stem cells of fetal or maternal origin from human placenta. *Stem Cells* **2004**, 22, 1338-1345.
- [5] Bieback K, Kern S, Klüter H, Eichler H. Critical parameters for the isolation of mesenchymal stem cells from umbilical cord blood. *Stem Cells* **2004**, 22, 625-634.
- [6] Jiang Y, Jahagirdar BN, Reinhardt RL, Schwartz RE, Keene CD, Ortiz-Gonzalez XR, Reyes M, Lenvik T, Lund T, Blackstad M, Du J, Aldrich S, Lisberg A, Low WC, Largaespada DA, Verfaillie CM. Pluripotency of mesenchymal stem cells derived from adult marrow. *Nature* **2002**, 418, 41-49.
- [7] Zuk PA, Zhu M, Ashjian P, De Ugarte DA, Huang JI, Mizuno H, Alfonso ZC, Fraser JK, Benhaim P, Hedrick MH. Human adipose tissue is a source of multipotent stem cells. *Mol Biol Cell* **2002**, 13, 4279-4295.
- [8] Komoda H, Okura H, Lee C-M, Sougawa N, Iwayama T, Hashikawa T, Saga A, Yamamoto-Kakuta A, Ichinose A, Murakami S, Sawa Y, Matsuyama A. Reduction of Neu5GC Xenoantigen on Human ADMSCs lead to Them as Safer and More Useful Cell Sources for Realizing Various Stem Cell Therapies. *Tissue Eng Part A*. **2010**, 16, 1143-1155.
- [9] Okura H, Matsuyama A, Lee CM, Saga A, Kakuta-Yamamoto A, Nagao A, Sougawa N, Sekiya N, Takekita K, Shudo Y, Miyagawa S, Komoda H, Okano T, Sawa Y. Cardiomyoblast-like cells differentiated from human adipose tissue-derived mesenchymal stem cells improve left ventricular dysfunction and survival in a rat myocardial infarction model. *Tissue Eng Part C Methods*. **2010**, 16, 417-425.
- [10] Okura H, Komoda H, Saga A, Yamamoto-Kakuta A, Fumimoto Y, Lee C-M, Ichinose A, Sawa Y, Matsuyama A. Properties of hepatocyte-like cell clusters from human adipose tissue-derived mesenchymal stem cells. *Tissue Eng Part C Methods*. **2010**, 16, 761-770.
- [11] Okura H, Fumimoto Y, Komoda H, Yanagisawa T, Nishida T, Noguchi S, Sawa Y., Matsuyama A. Transdifferentiation of Human Adipose Tissue-Derived Stromal Cells into Insulin-Producing Clusters. *J Artif Organs*. **2009**, 12, 123-130.
- [12] Okura H, Saga A, Fumimoto Y, Soeda M, Moriyama M, Moriyama H, Nagai K, Lee CM, Yamashita S, Ichinose A, Hayakawa T, Matsuyama A. Transplantation of human adipose tissue-derived multilineage progenitor cells reduces serum cholesterol in hyperlipidemic Watanabe rabbits. *Tissue Eng Part C Methods*. **2011**, 17, 145-154.
- [13] Saga A, Okura H, Soeda M, Tani J, Fumimoto Y, Komoda H, Moriyama M, Moriyama H, Yamashita S, Ichinose A, Daimon T, Hayakawa T, Matsuyama A. HMG-CoA reductase inhibitor augments the serum total cholesterol-lowering effect of human adipose tissue-derived multilineage progenitor cells in hyperlipidemic homozygous Watanabe rabbits. *Biochem Biophys Res Commun*. **2011**, 412, 50-54.
- [14] Hosono T, Mizuguchi H, Katayama K, Koizumi N, Kawabata K, Yamaguchi T, Nakagawa S, Watanabe Y, Mayumi T, Hayakawa T. RNA interference of PPARgamma using fiber-modified adenovirus vector efficiently suppresses preadipocyte-to-adipocyte differentiation in 3T3-L1 cells. *Gene* **2005**, 348, 157-165.
- [15] Yanagita M, Kashiwagi Y, Kobayashi R, Tomoeda M, Shimabukuro Y, Murakami S. Nicotine inhibits mineralization of human dental pulp cells. *J Endod*. **2008**, 34, 1061-1065.
- [16] Katz AJ, Llull R, Hedrick MH, Futrell JW. Emerging approaches to the tissue engineering of fat. *Clin Plast Surg* **1999**, 26, 587-603
- [17] Rodbell M. Metabolism of isolated fat cells. II. The similar effects of phospholipase c (*Clostridium perfringens* alpha toxin) and of insulin on glucose and amino acid metabolism. *J Biol Chem*. **1966**, 241, 130-139.
- [18] Rodbell M. The metabolism of isolated fat cells. IV. Regulation of release of protein by lipolytic hormones and insulin. *J Biol Chem*. **1966**, 241, 3909-3917.
- [19] Rodbell M, Jones AB. Metabolism of isolated fat cells. III. The similar inhibitory action of phospholipase c (clostridium perfringens alpha toxin) and of insulin on lipolysis stimulated by lipolytic hormones and theophylline. *J Biol Chem*. **1966**, 241, 140-142.
- [20] Van RL, Bayliss CE, Roncari DA. Cytological and enzymological characterization of adult human adipocyte precursors in culture. *J Clin Invest*. **1976**, 58, 699-704.
- [21] Björntorp P, Karlsson M, Gustafsson L, Smith U, Sjöström L, Cigolini M, Storck G, Pettersson P. Quantitation of different cells in the epididymal fat pad of the rat. *J Lipid Res*. **1979**, 20, 97-106
- [22] Deslex S, Negrel R, Vannier C, Etienne J, Ailhaud G. Differentiation of human adipocyte precursors in a chemically defined serum-free medium. *Int J Obes*. **1987**, 11, 19-27.
- [23] Hauner H, Entenmann G, Wabitsch M, Gaillard D, Ailhaud G, Negrel R, Pfeiffer EF. Promoting effect of glucocorticoids on the differentiation of human adipocyte precursor cells cultured in a chemically defined medium. *J Clin Invest*. **1989**, 84, 1663-1670.
- [24] Björntorp P, Karlsson M, Pertoft H, Pettersson P, Sjöström L, Smith U. Isolation and characterization of cells from rat adipose tissue developing into adipocytes. *J Lipid Res*. **1978**, 19, 316-324.
- [25] Yamanaka S. Strategies and new developments in the generation of patient-specific pluripotent stem cells. *Cell Stem Cell*. **2007**, 1, 39-49.
- [26] Gurdon JB, Melton DA. Nuclear reprogramming in cells. *Science* **2008**, 322, 1811-1815.

Reduction of *N*-Glycolylneuraminic Acid Xenoantigen on Human Adipose Tissue-Derived Stromal Cells/Mesenchymal Stem Cells Leads to Safer and More Useful Cell Sources for Various Stem Cell Therapies

Hiroshi Komoda, M.D., Ph.D.,^{1,2,*} Hanayuki Okura, M.S.,^{1,3,4,*} Chun Man Lee, M.D., Ph.D.,^{1,5} Nagako Sougawa, D.M.D., Ph.D.,¹ Tomoaki Iwayama, D.M.D.,⁶ Tomoko Hashikawa, D.M.D., Ph.D.,⁶ Ayami Saga, M.S.,¹ Aya Yamamoto-Kakuta, B.S.,¹ Akihiro Ichinose, M.D., Ph.D.,⁷ Shinya Murakami, D.M.D., Ph.D.,⁶ Yoshiki Sawa, M.D., Ph.D.,^{3,5} and Akifumi Matsuyama, M.D., Ph.D.¹

Adipose tissue is an attractive source for somatic stem cell therapy. Currently, human adipose tissue-derived stromal cells/mesenchymal stem cells (hADSCs/MSCs) are cultured with fetal bovine serum (FBS). Recently, however, not only human embryonic stem cell lines cultured on mouse feeder cells but also bone marrow-derived human MSCs cultured with FBS were reported to express *N*-glycolylneuraminic acid (Neu5Gc) xenoantigen. Human serum contains high titers of natural preformed antibodies against Neu5Gc. We studied the presence of Neu5Gc on hADSCs/MSCs cultured with FBS and human immune response mediated by Neu5Gc. Our data indicated that hADSCs/MSCs cultured with FBS expressed Neu5Gc and that human natural preformed antibodies could bind to hADSCs/MSCs. However, hADSCs/MSCs express complement regulatory proteins such as CD46, CD55, and CD59 and are largely resistant to complement-mediated cytotoxicity. hADSCs/MSCs cultured with FBS could be injured by antibody-dependent cell-mediated cytotoxicity mechanism. Further, human monocyte-derived macrophages could phagocytose hADSCs/MSCs cultured with FBS and this phagocytic activity was increased in the presence of human serum. Culturing hADSCs/MSCs with heat-inactivated human serum for a week could markedly reduce Neu5Gc on hADSCs/MSCs and prevent immune responses mediated by Neu5Gc, such as binding of human natural preformed antibodies, antibody-dependent cell-mediated cytotoxicity, and phagocytosis. Adipogenic and osteogenic differentiation potentials of hADSCs/MSCs cultured with heat-inactivated human serum were not less than that of those cultured with FBS. For stem cell therapies based on hADSCs/MSCs, hADSCs/MSCs that presented Neu5Gc on their cell surfaces after exposure to FBS should be cleaned up to be rescued from xenogeneic rejection.

Introduction

ADIPPOSE TISSUE is an attractive source for somatic cell therapy, because it is safe and abundant and many investigators have reported that the stromal cells derived from adipose tissue (adipose tissue-derived stromal cells [ADSCs]) could differentiate into various cell types.¹⁻⁴ ADSCs are also referred to as adipose tissue-derived mesenchymal

stem cells (MSCs). Human ADSCs (hADSCs)/MSCs are very similar to bone marrow (BM)-derived human MSCs (hMSCs) and therefore reveal differentiation potential similar to BM-derived hMSCs.⁵⁻⁷

For stem cell therapies based on hMSCs including hADSCs/MSCs, it is essential that stem cells are handled and cultured in a manner that guarantees the efficacy and safety of the cellular therapy product. One such aspect is the choice

¹Department of Somatic Stem Cell Therapy, Foundation for Biomedical Research and Innovation, Kobe, Hyogo, Japan.

²Department of Internal Medicine, National Hospital Organization Chiba Medical Center, Chiba, Japan.

³Department of Surgery, Osaka University Graduate School of Medicine, Suita, Osaka, Japan.

⁴Japan Society for the Promotion of Science, Tokyo, Japan.

⁵Medical Center for Translational Research, Osaka University Hospital, Suita, Osaka, Japan.

⁶Department of Periodontology, Division of Oral Biology and Disease Control, Osaka University Graduate School of Dentistry, Osaka, Japan.

⁷Department of Plastic Surgery, Kobe University Hospital, Kobe, Hyogo, Japan.

*These authors contributed equally to this work.

of cell culture medium and supplements. In principle, most investigators agree that all animal materials should be avoided to maximize product safety. Currently, however, hADSCs/MSCs are cultured with fetal bovine serum (FBS), and the clinical efficacy of BM-derived hMSCs in human disease has been investigated using hMSCs cultured with FBS in a number of clinical trials.^{8–12}

Recently, not only human embryonic stem cell (hESC) lines cultured on mouse feeder cells but also BM-derived hMSCs cultured with FBS were reported to express *N*-glycolylneuraminic acid (Neu5Gc) xenoantigen,^{13,14} the so-called Hanganutziu–Deicher antigen.¹⁵ Humans are incapable of synthesizing the common mammalian sialic acid, Neu5Gc, because of an *Alu* transposon-mediated inactivation of the CMP-*N*-acetylneuraminic acid hydroxylase gene.^{16,17} Despite this, both hESC lines and BM-derived hMSCs were reported to express the Neu5Gc, apparently originating from the mouse feeder layers, animal-derived components, and FBS.^{13,14} The significant levels of Neu5Gc found on the surface of hESCs and hMSCs evidently originate from a Trojan Horse pathway involving endocytosis of extracellular glycoconjugates, delivery to the lysosome, release of Neu5Gc by lysosomal sialidase, active transport to the cytoplasm through the lysosomal sialic acid transporter, activation by CMP, and addition to nascent glycoproteins and glycolipids in the secretory pathway.¹⁸ It is also possible that amphipathic molecules carrying Neu5Gc might be directly transferred into the hESC and hMSC plasma membranes.¹⁹ Human serum contains high titers of natural preformed antibodies against Neu5Gc xenoantigen.^{20–22} Thus, binding of these natural preformed antibodies may lead to immune responses such as complement-mediated cytotoxicity (CMC), antibody-dependent cell-mediated cytotoxicity (ADCC), and antibody-dependent cellular phagocytosis. However, these immune responses mediated by natural preformed antibodies against human stem cells remain in controversy.^{13,23} This study was therefore undertaken to study the presence of Neu5Gc on hADSCs/MSCs cultured with FBS and the human immune responses mediated by Neu5Gc on hADSCs/MSCs.

Materials and Methods

Cells

hADSCs/MSCs were prepared as described previously^{1,2} with modifications.^{3,4} Adipose tissue was resected during plastic surgery in five human subjects (four men and one woman; age, 20–60 years) as excess discards. Ten to 50 g of

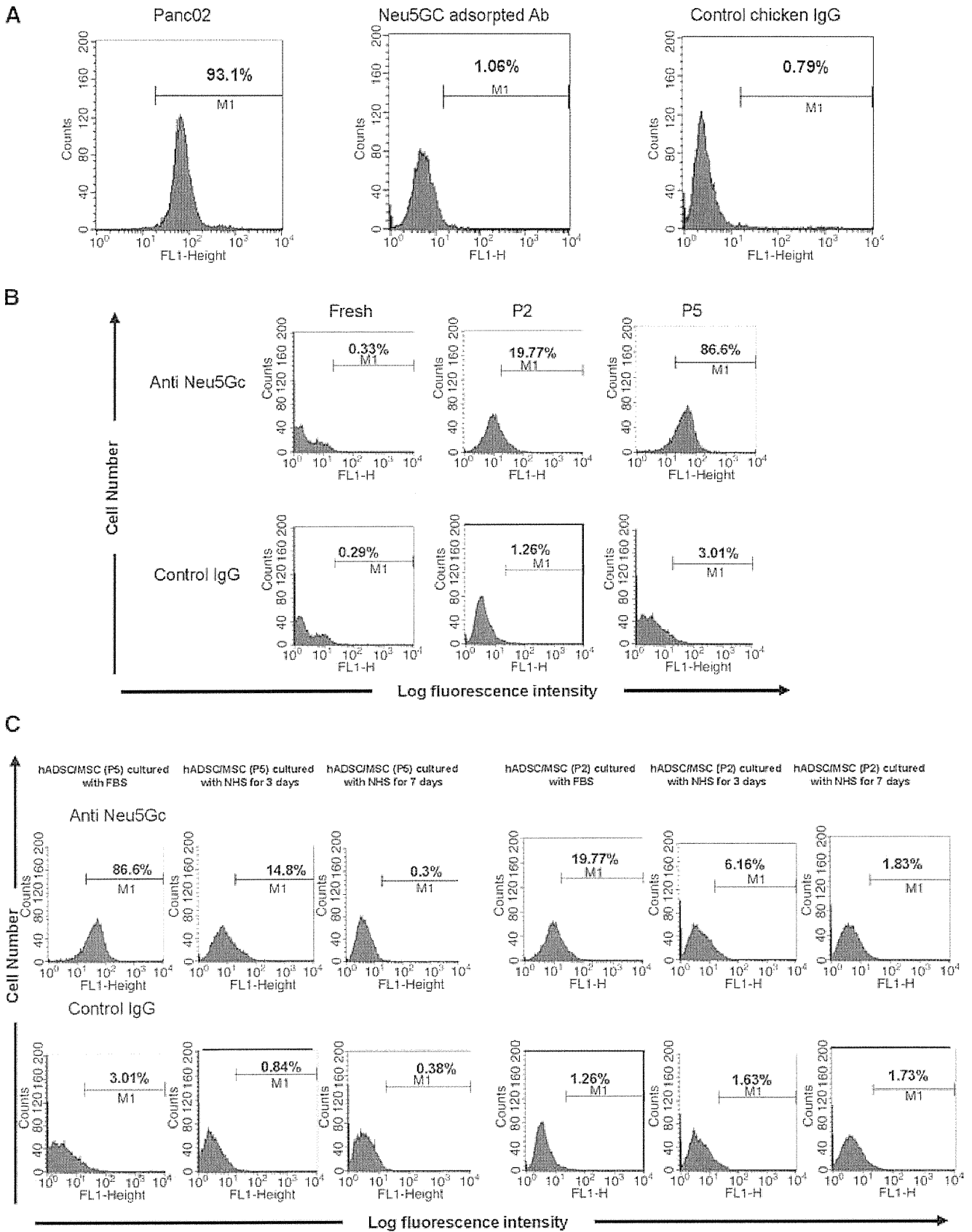
subcutaneous adipose tissue was collected from each subject. All subjects provided informed consent. The protocol was approved by the Review Board for Human Research of the Kobe University Graduate School of Medicine, Osaka University Graduate School of Medicine and Foundation for Biomedical Research and Innovation. All subjects fasted for at least 10 h before surgery and none was being treated with steroids. The resected excess adipose tissue was minced and then digested in Hank's balanced salt solution (Gibco Invitrogen, Grand Island, NY) containing 0.075% collagenase type II (Sigma Aldrich, St. Louis, MO) at 37°C for 1 h. Digests were filtered with a cell strainer (BD Bioscience, San Jose, CA) and centrifuged at 800 g for 10 min. Erythrocytes were excluded using density gradient centrifugation with Lymphoprep ($d = 1.077$; Nycomed, Oslo, Norway). The cells were then plated using Dulbecco's modified Eagle's medium (DMEM; Gibco Invitrogen) with 10% defined FBS (Hyclone) and incubated for 24 h at 37°C. Following incubation, the adherent cells were washed extensively and treated with 0.2 g/L ethylenediaminetetraacetate (EDTA) solution (Nacalai Tesque, Kyoto, Japan), and the resulting suspended cells were replated at a density of 10,000 cells/cm² on human fibronectin-coated dishes (BD BioCoat) in a medium containing 60% DMEM-low glucose, 40% MCDB-201 medium (Sigma Aldrich), 1×insulin–transferrin–selenium (Gibco Invitrogen), 1 nM dexamethasone (Sigma Aldrich), 100 μM ascorbic acid 2-phosphate (Sigma Aldrich), 10 ng/mL epidermal growth factor (PeproTec, Rocky Hill, NJ), and 5% FBS. For analysis of the effects of human serum on Neu5Gc expression on hADSCs/MSCs, the cells were cultured for 7 days, where FBS was replaced by 5% heat-inactivated normal human pooled serum (NHS) from type AB blood. As control cells, a murine pancreatic cell line, Panc02, was cultured with RPMI 1640 medium (Gibco Invitrogen) supplemented with 10% FBS and 1% antibiotic/antimycotic solution.

Flow cytometry

Cells were detached from culture dishes and suspended in Dulbecco's phosphate-buffered saline (D-PBS; Nacalai Tesque). Aliquots (5×10^5 cells) were incubated for 30 min at 4°C with a chicken anti-Neu5Gc polyclonal antibody (a gift from Prof. N. Wakamiya, Asahikawa Medical College, Hokkaido, Japan).²⁴ Cells incubated with D-PBS alone were used as negative control. After washing with D-PBS, cells were stained with fluorescein isothiocyanate (FITC)-conjugated rabbit anti-chicken immunoglobulin G (IgG; Cappel) as a second antibody. After staining, the cells were washed and resuspended

FIG. 1. Expression of Neu5Gc on hADSCs/MSCs. (A) Specificity of anti-Neu5Gc antibody. Panc02, a cell line derived from murine pancreatic carcinomas, expressed Neu5Gc. Flow cytometric analysis showed that chicken anti-Neu5Gc polyclonal antibody bound to the surfaces of Panc02, but Neu5Gc-preadsorbed anti-Neu5Gc polyclonal antibody could not react, showing specificity of the anti-Neu5Gc antibody. The percentage of cells that stained positive is indicated in the upper right corner of each panel. (B) Expression of Neu5Gc xenoantigen on hADSCs/MSCs. Fresh hADSCs/MSCs did not express Neu5Gc on their cell surface. In accordance with passage numbers, the population of Neu5Gc-positive cells increased by cultivation with FBS. The percentage of cells that stained positive is indicated in the upper right corner of each panel. (C) Reduction of Neu5Gc xenoantigen by chasing cultivation with human serum. After cultivation of hADSCs/MSCs with heat-inactivated NHS but not FBS, the percentages of Neu5Gc-positive cells have decreased in accordance with culture duration. The decrement manners of second passaged hADSCs/MSCs and fifth passaged ones have been in a similar fashion. The percentage of cells that stained positive is indicated in the upper right corner of each panel. Data are representative of four independent experiments. Neu5Gc, *N*-glycolylneuraminic acid; hADSCs/MSCs, human adipose tissue-stromal cells/mesenchymal stem cells; FBS, fetal bovine serum; NHS, normal human pooled serum; IgG, immunoglobulin G; M1; FL1.

HUMAN MESENCHYMAL STEM CELLS EXPRESS Neu5Gc XENOANTIGEN



in D-PBS with 150 ng/mL 7-AAD (BD Pharmingen) to eliminate dead cells. The cells were analyzed by flow cytometry using a FACSCalibur flow cytometer and CellQuest Pro software (BD Biosciences). Data shown in figures are gated for live cells by excluding cells that stained positive for 7-AAD. Percentage of positive cells was defined against a 99% negative control exclusion gate. For detection of binding of human natural preformed antibodies, the cells were exposed to 10% fresh NHS or 5 mM Neu5Gc-adsorbed NHS in D-PBS containing 15 mM EDTA for 30 min at 4°C. After washing, the cells were stained with FITC-conjugated goat anti-human IgG or IgM antibody (Cappel), or control goat IgG, respectively. To examine the blocking effects of anti-Neu5Gc antibody onto the surface of hADSCs/MSCs, hADSCs/MSCs cultured with FBS were precoated with anti-Neu5Gc antibody, exposed to 10% fresh NHS containing 15 mM EDTA, and then applied for flow cytometric analysis. Stained cells were washed and resuspended in D-PBS with 7-AAD and analyzed by a FACSCalibur flow cytometer. For detection of human complement regulatory proteins, cells were stained with FITC-conjugated mouse monoclonal antibodies to human CD46 (membrane cofactor protein), CD55 (decay accelerating factor), CD59, or control IgG (all from BD Pharmingen) and analyzed by a FACSCalibur flow cytometer as well.

Detection of complement deposition

The amounts of C4 and C3 fragments deposited on the cell surface were also analyzed by flow cytometry. The cells were detached by 0.25% trypsin/EDTA and subsequently incubated with 10% fresh NHS in DMEM for 30 min at 37°C. Cells incubated with DMEM alone or 10% fresh NHS in DMEM containing 15 mM EDTA was used as negative control. After washing with cold D-PBS three times, the cells were stained with FITC-conjugated rabbit anti-human C4c or C3c antibody (Dako). After staining, the cells were washed and resuspended in 500 μ L of D-PBS with 7-AAD and analyzed by a FACSCalibur flow cytometer.

CMC assay

CMC was evaluated by measuring lactate dehydrogenase (LDH) release in media, using MTX-LDH kit (Kyokuto

Pharm) in accordance with the manufacturer's instructions. Target cells (hADSCs/MSCs cultured with FBS, hADSCs/MSCs cultured with heat-inactivated NHS, or Panc02) were plated at a concentration of 1×10^4 cells/well in a 96-well culture plate. Then, DMEM with 20% or 40% fresh NHS was added. The plates were incubated for 2 h at 37°C, and LDH release was determined. All assays included maximal release controls (1% Triton X), controls with medium and target cells, with medium containing fresh NHS, and with medium alone.

Isolation of effector cells

Peripheral blood mononuclear cells (PBMCs) were isolated from the buffy coats from healthy volunteers using density gradient centrifugation with Lymphoprep (Nycomed). Cell viability was more than 98%, as determined by trypan blue exclusion. Human monocyte-derived macrophages were isolated and cultured as reported previously.²⁵

ADCC assay

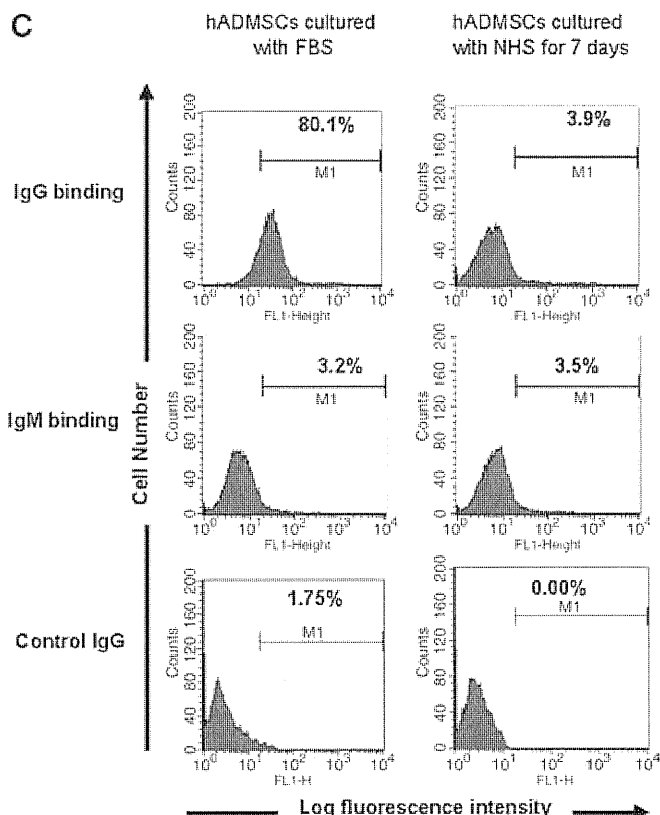
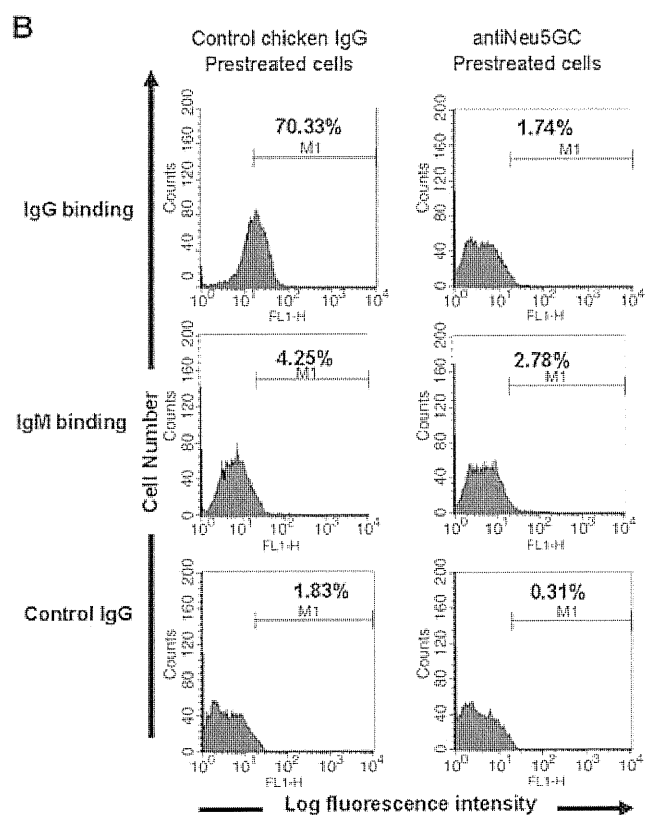
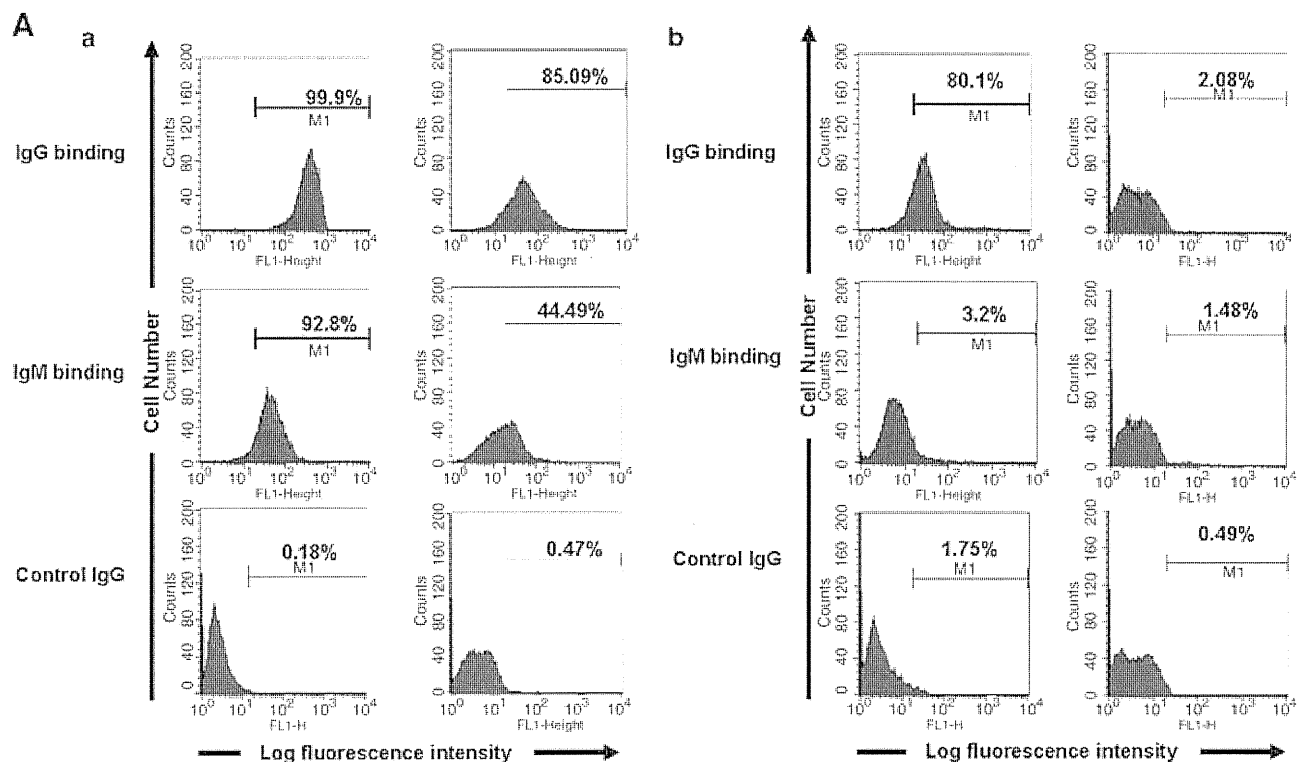
ADCC was also determined by measuring LDH release into medium. Target cells (hADSCs/MSCs cultured with FBS, hADSCs/MSCs cultured with heat-inactivated NHS, or Panc02) were plated in 96-well culture plates as described earlier. Then, 1×10^5 or 2×10^5 PBMCs in DMEM alone or with 10% heat-inactivated NHS were added. The plates were incubated for 4 h at 37°C, and LDH release was determined. All assays included maximal release controls (1% Triton X), controls with medium and target cells, with medium and effector cells, with medium containing 10% heat-inactivated NHS, and with medium alone.

Phagocytosis assay

Target cells (hADSCs/MSCs cultured with FBS, hADSCs/MSCs cultured with heat-inactivated NHS, or Panc02) were stained with PKH67 Green Fluorescent Cell Linker Mini Kit (Sigma Aldrich) according to the manufacturer's instructions. After labeling of target cells was terminated, the cells were washed and resuspended in RPMI medium. Then, 2×10^6 PKH67-labeled target cells were added into 24-well culture plates and incubated with 2×10^5 human

FIG. 2. Binding of natural preformed antibodies to hADSCs/MSCs. (A) Binding of natural preformed antibodies to Panc02 and hADSCs/MSCs. (a) Murine pancreatic carcinoma cell line Panc02 was exposed to 10% fresh NHS containing 15 mM EDTA, then stained with secondary FITC-conjugated goat anti-human IgG or IgM antibody, and studied by flow cytometry to demonstrate the binding of IgG and IgM. The natural performed antibodies human IgG and IgM bound onto Panc02. Exposition of Neu5Gc-adsorbed NHS could reduce the natural performed antibody binding (IgG binding: 99.95% to 85.09%; IgM binding: 92.8% to 44.49%). (b) hADSCs/MSCs were cultured with FBS, exposed to 10% fresh NHS containing 15 mM EDTA, and then stained with secondary FITC-conjugated goat anti-human IgG or IgM antibody, or control goat IgG. The natural performed antibodies human IgG and IgM bound onto hADSCs/MSCs, and exposition of Neu5Gc-adsorbed NHS could reduce IgG binding (80.01% to 2.08%). The percentage of cells that stained positive is indicated in the upper right corner of each panel. Data are representative of four independent experiments. (B) Anti-Neu5Gc antibody pretreatment suppressed the binding of natural preformed antibodies onto hADSCs/MSCs. hADSCs/MSCs cultured with FBS were precoated with anti-Neu5Gc antibody and then exposed to 10% fresh NHS containing 15 mM EDTA. The natural performed antibody human IgG bound onto hADSCs/MSCs, and exposition of anti-Neu5Gc antibody could reduce IgG binding (70.33% to 1.74%). The percentage of cells that stained positive is indicated in the upper right corner of each panel. Data are representative of three independent experiments. (C) Decrement of binding of natural preformed antibodies onto hADSCs/MSCs by chase with NHS. After cultivation of hADSCs/MSCs with heat-inactivated NHS but not FBS, the percentages of human IgG-positive cells decreased. The percentage of cells that stained positive is indicated in the upper right corner of each panel. Data are representative of four independent experiments. hADMSCs; EDTA, ethylenediaminetetraacetate; FITC, fluorescein isothiocyanate.

HUMAN MESENCHYMAL STEM CELLS EXPRESS Neu5Gc XENOANTIGEN



monocyte-derived macrophages ($E:T = 1:10$) in 1 mL of RPMI 1640 medium alone or with 10% heat-inactivated NHS for 24 h at 37°C. Following incubation, the target cells and human monocyte-derived macrophages were harvested with EDTA solution. The cells were counterstained with allophycocyanin-conjugated mouse monoclonal antibodies to human CD11c (BD Pharmingen) and washed and fixed with 2% formaldehyde-PBS. Two-color flow cytometric analysis was performed with a FACSCalibur flow cytometer under optimal gating. PKH67-labeled target cells were detected in the FL-1 channel and allophycocyanin-labeled human monocyte-derived macrophages were detected in the FL-4 channel. Dual-labeled cells (PKH67⁺/CD11c⁺) were considered to represent phagocytosis of targets by human monocyte-derived macrophages. Residual target cells were defined as cells that were PKH67⁺/CD11c⁺.

Adipogenic and osteogenic differentiation procedure

For adipogenic differentiation, cells were cultured in differentiation medium (Zen-Bio). After 3 days, half of the medium was changed with adipocyte medium (Zen-Bio) every 2 days. Ten days after differentiation, characterization of adipocytes was confirmed by microscopic observation of intracellular lipid droplets by oil red O staining. Osteogenic differentiation was induced by culturing the cells in DMEM containing 10 nM dexamethasone, 50 mg/dL ascorbic acid 2-phosphate, 10 mM beta-glycerophosphate (Sigma), and 10% FBS or heat-inactivated NHS. The differentiation was examined by alizarin red staining and alkaline phosphatase (AP) activity. For alizarin red staining, 7 or 18 days after differentiation, the cells were washed three times and fixed with dehydrated ethanol. After fixation, the cells were stained with 1% alizarin red S in 0.1% NH₄OH (pH 6.5) for 5 min and then washed with H₂O. AP activity was investigated at 2 weeks after differentiation using the procedure described previously.²⁶ AP activity per cell was calculated based on the amount of DNA. DNA content was measured by a modification of the method of Labarca and Paigen.²⁷

Statistics

Values are given as the mean ± standard deviation. Student's *t*-test was used to ascertain the significance of differences within groups. Differences were considered statistically significant when $p < 0.05$. All statistical analyses were performed using the SPSS Statistics 17.0 package (SPSS, Chicago, IL).

Results

Presence of Neu5Gc and human natural preformed antibodies binding to hADSCs/MSCs

First, the specificity of chicken anti-Neu5Gc polyclonal antibody was examined (Fig. 1A). Flow cytometric analysis showed that chicken anti-Neu5Gc polyclonal antibody bound to the surfaces of Panc02, which constitutively expressed Neu5Gc, but Neu5Gc-preadsorbed anti-Neu5Gc polyclonal antibody could not react, indicating the anti-Neu5Gc antibody reacts to Neu5Gc specifically. Next, incorporation of Neu5Gc antigen via FBS-containing medium was examined (Fig. 1B). Fresh hADSCs/MSCs did not express Neu5Gc on their cell surface. In accordance with passage numbers, the

population of Neu5Gc-positive cells has increased by cultivation with FBS (fresh: 0.33%; passage number 2: 19.77%; and passage number 5: 86.6%). Culture with heat-inactivated NHS could markedly reduce Neu5Gc in human colon carcinoma cells,²² hESCs,¹³ and hMSCs,¹⁴ apparently as the result of metabolic replacement by *N*-acetylneuraminic acid in the human serum. So, the reduction of incorporated Neu5Gc xenoantigen by chasing cultivation with human serum was examined (Fig. 1C). The Neu5Gc xenoantigen was reduced after cultivation of hADSCs/MSCs with heat-inactivated NHS but not FBS. The percentages of Neu5Gc-positive cells have decreased in accordance with culture duration, and the decrement manners of second passaged hADSCs/MSCs and fifth passaged ones have been in a similar fashion.

Because human serum contains high titers of natural preformed antibodies against the Neu5Gc xenoantigen,^{20–22} we assessed whether such antibodies could recognize Neu5Gc-containing epitopes on hADSCs/MSCs cultured with FBS (Fig. 2). Panc02 cultured with FBS and exposed to 10% fresh NHS containing 15 mM EDTA showed high human IgG (99.9%) and IgM (92.8%) binding (Fig. 2Aa). hADSCs/MSCs cultured with FBS and treated with fresh NHS also showed high human IgG binding (80.1%), but human IgM binding was very low (3.2%) (Fig. 2Ab). Preincubation of fresh NHS with Neu5Gc resulted in significant decrease in human IgG binding on hADSCs/MSCs cultured with FBS (80.1% to 2.08%). Further, pretreatment of hADSCs/MSCs with anti-Neu5Gc polyclonal antibody also resulted in reduction of human IgG binding (70.33% to 1.74%; Fig. 2B). Culturing hADSCs/MSCs with heat-inactivated NHS, which decreased Neu5Gc expression of hADSCs/MSCs effectively, reduced human IgG binding on hADSCs/MSCs when exposed to fresh NHS (Fig. 2C). Taken together, these data indicate that the hADSCs/MSCs cultured with FBS expressed Neu5Gc and the human natural preformed antibodies could bind to hADSCs/MSCs. This binding of human natural preformed antibodies on hADSCs/MSCs was related to the amount of Neu5Gc on hADSCs/MSCs. Culture with heat-inactivated NHS could markedly reduce IgG binding on hADSCs/MSCs when exposed to fresh NHS (80.1% to 3.9%).

Complement fragment deposition on hADSCs/MSCs and CMC assay

Cell surface antibody binding may activate the classical complement pathway leading to cytotoxicity. We assessed whether the deposition of complement fragments on hADSCs/MSCs occurred after exposure to fresh NHS. Whether hADSCs/MSCs were cultured with FBS or heat-inactivated NHS, the amount of deposition of C4 and C3 fragments on hADSCs/MSCs after a short incubation period of 30 min was no different from negative control (cells incubated with DMEM alone or 10% fresh NHS in DMEM containing 15 mM EDTA) (Fig. 3). To control for fresh NHS activity and variability, we tested the deposition of C4 and C3 fragments on Panc02. Both complement fragments were clearly deposited on Panc02 (C4: 84.6%; C3: 98.99%) and this deposition was abolished by adding 15% EDTA (Fig. 3). We next analyzed the CMC of hADSCs/MSCs cultured with FBS or heat-inactivated NHS. To control for CMC of fresh NHS, we tested CMC of Panc02. CMC of Panc02 was clearly detected (20% NHS: 42.7% ± 4.7%; 40% NHS: 65.4% ± 2.4%).

HUMAN MESENCHYMAL STEM CELLS EXPRESS Neu5Gc XENOANTIGEN

7

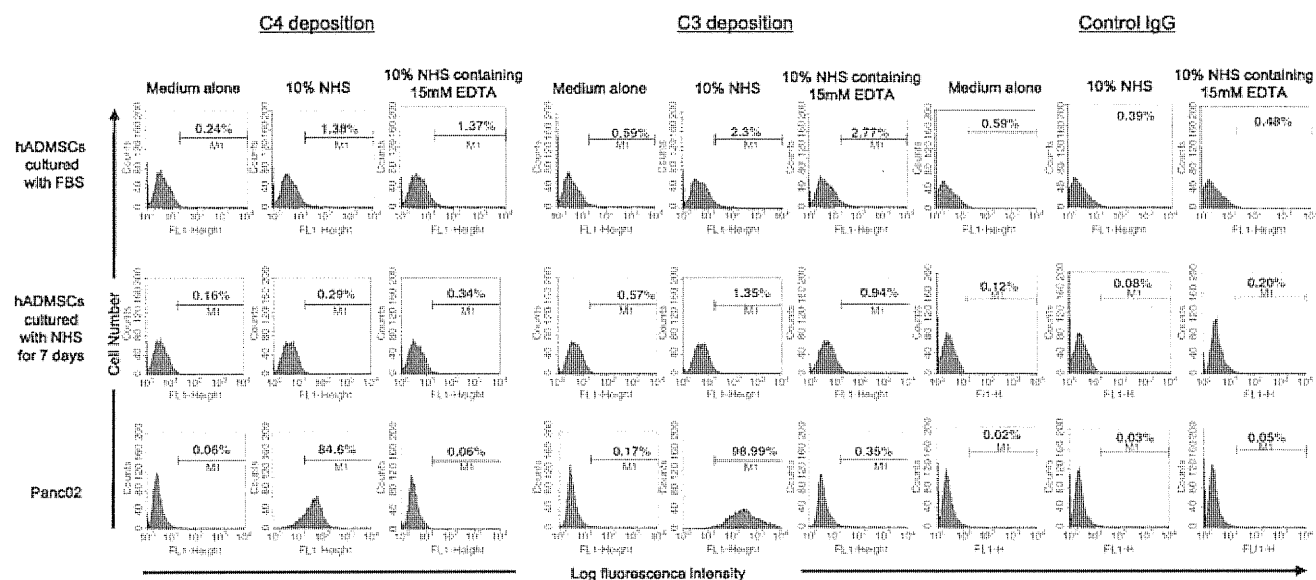


FIG. 3. Complement deposition onto hADSCs/MSCs by NHS. The cells were exposed to medium alone, 10% NHS, or 10% NHS containing 15 mM EDTA, followed by an analysis of deposition of complement fragments C4 and C3. The percentage of cells that stained positive is indicated in the upper right corner of each panel. Data are representative of four independent experiments.

In contrast, significant specific lysis of hADSCs/MSCs cultured with FBS or heat-inactivated NHS was not detected (hADSCs/MSCs cultured with FBS + 20% NHS: $4.8\% \pm 1.3\%$; or 40% NHS: $7.4\% \pm 2.0\%$; hADSCs/MSCs cultured with heat-inactivated NHS: 20% NHS: $3.6\% \pm 1.6\%$; 40% NHS: $5.6\% \pm 1.6\%$). We then analyzed the expression of complement regulatory proteins such as CD46, CD55, and CD59 on hADSCs/MSCs. hADSCs/MSCs were weakly positive for both CD46 (22.1%) and CD55 (29.8%) and highly positive for CD59 (97.5%) (Fig. 4B). These data indicate that hADSCs/MSCs express complement regulatory proteins such as CD46, CD55, and CD59 and are largely resistant to killing by CMC mechanism.

ADCC of hADSCs/MSCs mediated by human natural preformed antibodies in NHS

IgG antibodies play an important role in ADCC.²⁸ Our study demonstrated that natural preformed IgG antibodies could bind to hADSCs/MSCs cultured with FBS. Therefore, to evaluate the role of these IgG antibodies in cell-mediated cytotoxicity, ADCC assay was performed with hADSCs/MSCs cultured with FBS, hADSCs/MSCs cultured with heat-inactivated NHS, or Panc02 as targets and human PBMCs as effector cells, using $E:T$ ratios of 10:1 and 20:1, and 4-h incubation periods. PBMCs in the absence of heat-inactivated NHS caused no significant lysis of hADSCs/MSCs cultured with FBS, hADSCs/MSCs cultured with heat-inactivated NHS, and Panc02 (hADSCs/MSCs cultured with FBS: $E:T = 10:1$, $2.37\% \pm 0.35\%$; $E:T = 20:1$, $3.78\% \pm 0.85\%$; hADSCs/MSCs cultured with heat-inactivated NHS: $E:T = 10:1$, $0.57\% \pm 0.36\%$; $E:T = 20:1$, $2.34\% \pm 0.67\%$; Panc02: $E:T = 10:1$, $1.98\% \pm 0.35\%$; $E:T = 20:1$, $4.7\% \pm 0.54$; Fig. 5, white bar). The cytotoxicity of Panc02 in the presence of heat-inactivated NHS was significantly greater than that in the absence of heat-inactivated NHS (in the presence of NHS vs. in the absence

of heat-inactivated NHS: $E:T = 10:1$, $27.4\% \pm 3.1\%$ vs. $1.98\% \pm 0.35\%$, $p < 0.05$; $E:T = 20:1$, $28.9\% \pm 4.6\%$ vs. $4.7 \pm 0.54\%$, $p < 0.05$), which proved the effective use of PBMCs (Fig. 5). A significant increase of cytotoxicity of the hADSCs/MSCs cultured with FBS was also evident in the presence of heat-inactivated NHS (in the presence of heat-inactivated NHS vs. in the absence of heat-inactivated NHS: $E:T = 10:1$, $13.5\% \pm 0.82\%$ vs. $2.37\% \pm 0.35\%$, $p < 0.05$; $E:T = 20:1$, $16.0\% \pm 1.5\%$ vs. $3.78\% \pm 0.85$, $p < 0.05$; Fig. 5). In contrast, no increase of cytotoxicity of the hADSCs/MSCs cultured with heat-inactivated NHS was detected in the presence of heat-inactivated NHS vs. in the absence of heat-inactivated NHS (in the presence of heat-inactivated NHS vs. in the absence of heat-inactivated NHS: $E:T = 10:1$, $3.23\% \pm 0.52\%$ vs. $0.57\% \pm 0.36\%$; $E:T = 20:1$, $3.75\% \pm 0.51\%$ vs. $2.34\% \pm 0.67\%$; Fig. 5). In addition, the cytotoxicity the hADSCs/MSCs cultured with FBS was significantly greater than that of hADSCs/MSCs cultured with heat-inactivated NHS which expressed negligible amount of Neu5Gc (hADSCs/MSCs cultured with FBS vs. hADSCs/MSCs cultured with heat-inactivated NHS: $E:T = 10:1$, $13.5\% \pm 0.82\%$ vs. $3.23\% \pm 0.52\%$, $p < 0.05$; $E:T = 20:1$, $16.0\% \pm 1.5\%$ vs. $3.75\% \pm 0.51$, $p < 0.05$; Fig. 5). Taken together, these data indicate that the hADSCs/MSCs cultured with FBS are injured by ADCC mechanism. In contrast, hADSCs/MSCs cultured with NHS are less sensitive to ADCC.

Phagocytosis of hADSCs/MSCs by human monocyte-derived macrophages

hADSCs/MSCs cultured with FBS, hADSCs/MSCs cultured with heat-inactivated NHS, or Panc02 were stained with fluorescent PKH67, respectively. Labeled cells were cocultured with human monocyte-derived macrophages in the presence or absence of heat-inactivated NHS for 24 h. After counterstaining with monoclonal antibodies to human CD11c, two-color flow cytometric analysis was performed

FIG. 4. Sensitivity of hADMSCs to lysis by NHS. **(A)** Complement-mediated cytotoxicity assay of hADMSCs/MSCs. The cytotoxic activity of 20% or 40% NHS against hADMSCs/MSCs was tested by lactate dehydrogenase release. Data are shown as mean \pm standard deviation. **(B)** Complement regulatory proteins on hADMSCs/MSCs were studied by flow cytometry using FITC-conjugated antibodies to human CD46, CD55, CD59, or control IgG. Data are representative of three independent experiments.

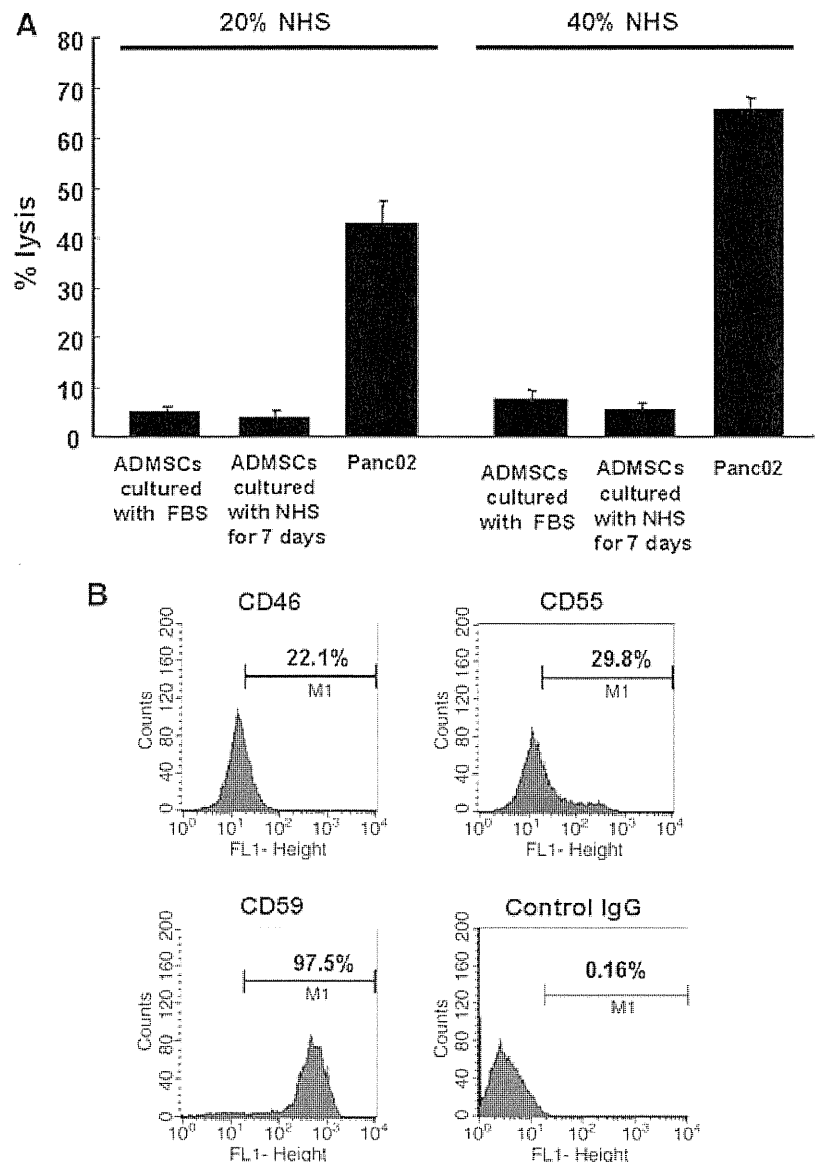


FIG. 6 (Fig. 6). Phagocytosis of target cells by human monocyte-derived macrophages could be identified as dual-labeled cells (PKH67⁺/CD11c⁺, right upper panel). Similar results were obtained in three independent experiments. Phagocytosis of Panc02 was clearly detectable (10.6%) and increased twofold in the presence of heat-inactivated NHS, which proved the effective use of human monocyte-derived macrophages. Phagocytosis of hADMSCs/MSCs cultured with NHS by human monocyte-derived macrophages was somewhat detectable (5.7%) and also increased in the presence of heat inactivated human serum (9.3%). In contrast, human monocyte-derived macrophages could not phagocytose hADMSCs/MSCs cultured with heat-inactivated NHS neither in the absence nor in the presence of heat-inactivated NHS (medium alone: 1.1%; 10% heat-inactivated NHS: 2.2%; Fig. 6). Thus, human monocyte-derived macrophages phagocytosed hADMSCs/MSCs cultured with FBS and this phagocytic activity increased when hADMSCs/MSCs cultured with FBS were opsonized by the natural preformed antibodies in the presence of heat-inactivated NHS. In contrast,

hADMSCs/MSCs cultured with heat-inactivated NHS were resistant to phagocytosis either in the absence or in the presence of heat-inactivated NHS.

Adipogenic and osteogenic differentiation potentials of hADMSCs/MSCs cultured with FBS and heat-inactivated NHS

To compare the *in vitro* differentiation potential of hADMSCs/MSCs cultured with FBS or heat-inactivated NHS, cells were differentiated toward the adipogenic and osteogenic lineages. Adipogenic differentiation was induced by culture with differentiation medium containing 1-methyl-3-isobutylxanthine, PPAR-gamma agonist, dexamethasone, and insulin. The acquisition of the adipogenic phenotype was determined by staining the cell monolayers with oil red O (Fig. 7A). The efficiency of adipogenesis of hADMSCs/MSCs cultured with heat-inactivated NHS was similar to that of hADMSCs/MSCs cultured with FBS (Fig. 7A). Both hADMSCs/MSCs showed multiple intracellular lipid-filled droplets in 35–50% of cells

HUMAN MESENCHYMAL STEM CELLS EXPRESS Neu5Gc XENOANTIGEN

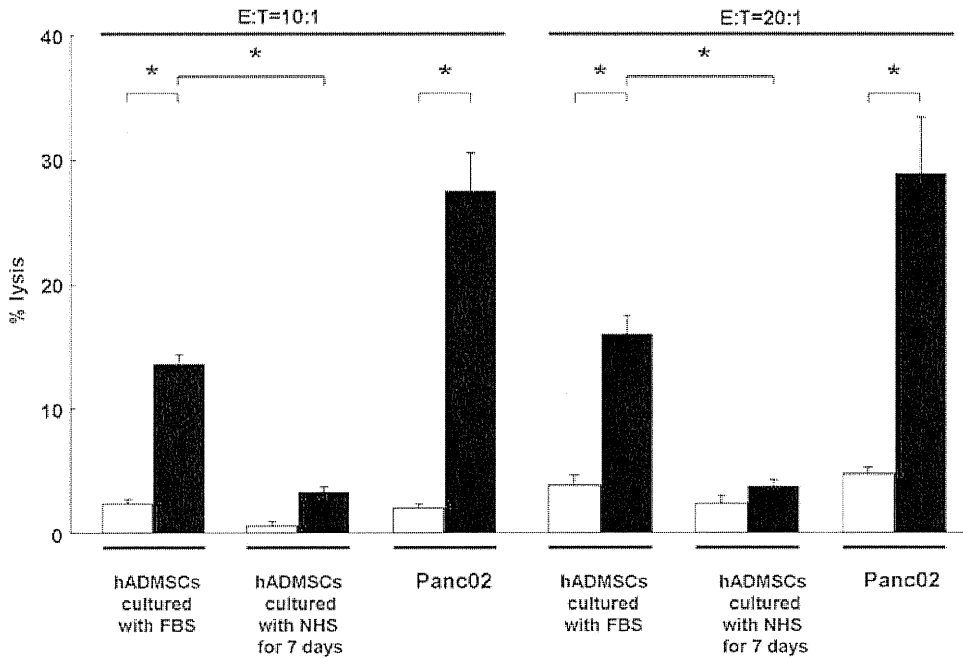


FIG. 5. Antibody-dependent cell-mediated cytotoxicity assay of hADSCs/MSCs. The cytotoxic activity of peripheral blood mononuclear cells against hADSCs/MSCs in the absence (white bar) or presence (black bar) of 10% NHS was tested by measuring lactate dehydrogenase release into medium (E:T = 10:1 or 20:1). Data are shown as mean ± standard deviation (*p < 0.05) and are representative of three independent experiments.

after adipogenic induction. Osteogenic differentiation was induced by treating cells with low concentrations of dexamethasone, ascorbic acid, and beta-glycerophosphate. Calcium deposition was demonstrated by staining monolayers with alizarin red (Fig. 7B). hADSCs/MSCs cultured with heat-

inactivated NHS and those cultured with FBS showed similar potential toward osteogenic differentiation. High AP activity was detected in hADSCs/MSCs cultured with heat-inactivated NHS and those cultured with FBS in response to osteogenic induction after 2 weeks (Fig. 7B).

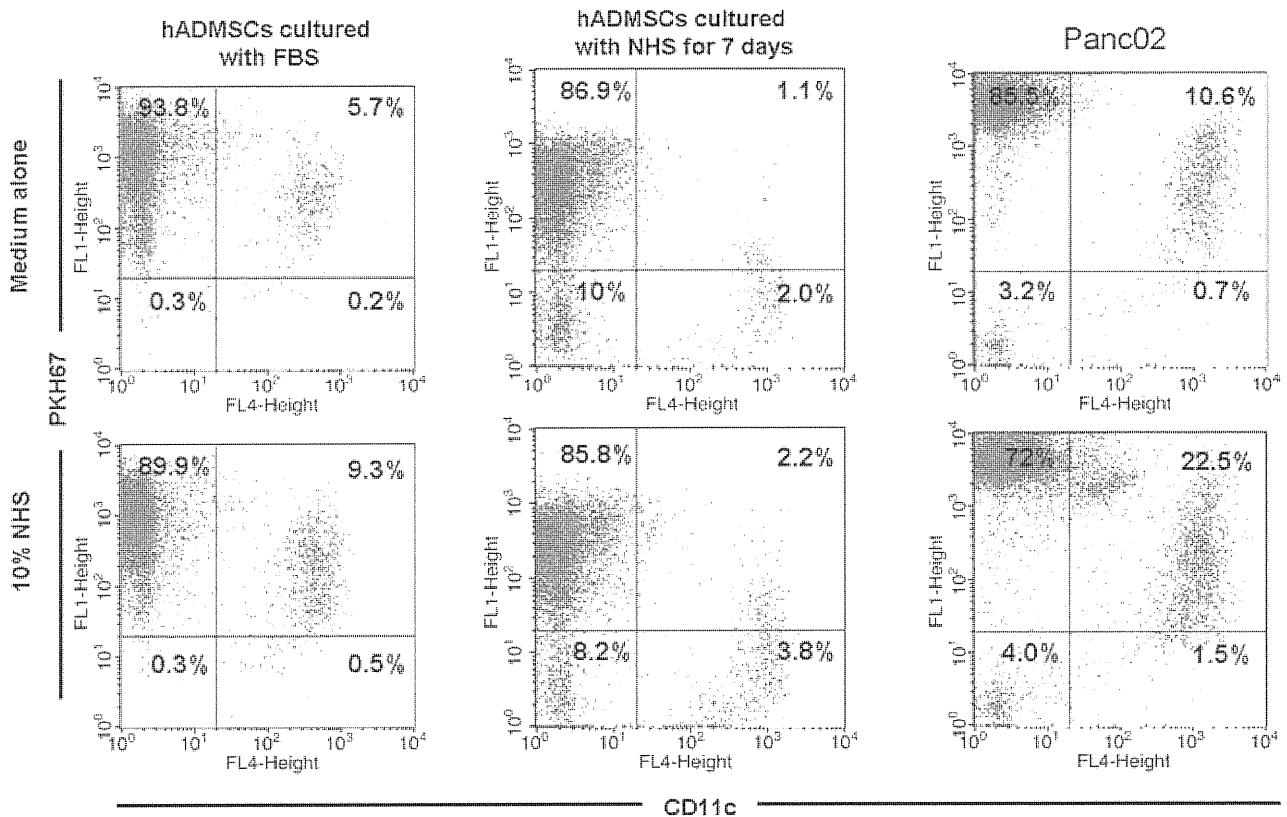


FIG. 6. Representative flow cytometry profiles of phagocytosis assay of hADSCs/MSCs. Upper left quadrant: Region of residual target cells. Upper right quadrant: Region of phagocytosed target cells. Percentages represent those of total cells in each region. Data are representative of three independent experiments.